ELSEVIER

Journal of Structural Geology 27 (2005) 2058–2083

JOURNAL OF STRUCTURAL GEOLOGY

www.elsevier.com/locate/jsg

Structural geology of a classic thrust belt earthquake: the 1999 Chi-Chi earthquake Taiwan ($M_w = 7.6$)

Li-Fan Yue[a,*], John Suppe[a], Jih-Hao Hung[b]

[a]*Department of Geosciences, Princeton University, Princeton, NJ 08544, USA*
[b]*Institute of Geophysics, National Central University, Chung-Li, Taiwan, ROC*

Received 26 April 2004; received in revised form 29 September 2004; accepted 24 May 2005
Available online 9 September 2005

Abstract

We document the structural context of the 1999 Chi-Chi earthquake ($M_w = 7.6$) in western Taiwan, which is one of the best-instrumented thrust-belt earthquakes. The main surface break and large slip (3–10 m) is on two segments of the shallow otherwise aseismic bedding-parallel Chelungpu–Sanyi thrust system, which shows nearly classic ramp-flat geometry with shallow detachments (1–6 km) in the Pliocene Chinshui Shale and Mio-Pliocene Kueichulin/Tungkeng Formations. However, rupture is complex, involving at least six faults, including a previously unknown deeper thrust (8–10 km) on which the rupture began. We compare the coseismic displacements with a new 3D map of the Chelungpu–Sanyi system. The displacements are spatially and temporally heterogeneous and well correlated with discrete geometric segments of the 3D shape of the fault system. Geodetic displacement vectors are statistically parallel to the nearest adjacent fault segment and are parallel to large-scale oblique fault corrugations. The displacement magnitudes are heterogeneous at several scales, which requires in the long term other non-Chi-Chi events or significant aseismic deformation. The Chelungpu thrust has a total displacement of ~14 km but the area of largest Chi-Chi slip (~10 m) is on a newly propagated North Chelungpu Chinshui detachment (~0.3 km total slip) which shows abnormally smooth rupture dynamics.

Keywords: Active tectonics; Thrust faulting; Coseismic displacement; Fault geometry; Chi-Chi earthquake; Taiwan

1. Introduction

It has been said that large earthquakes are the quanta of upper crustal structural geology, making them focal points in studies of active tectonics (King et al., 1988; Stein et al., 1988; Yeats et al., 1996). Many structures grow largely by the summation of a few thousand large earthquakes, with 1–10 m growth per earthquake (Stein and King, 1984). Unfortunately, the subsurface structural geology of large earthquakes is normally only rather weakly constrained, making it difficult to form robust relationships between the displacements in large earthquakes—as constrained by geodesy, seismology and geomorphology—and the subsurface fault and fold geometry. The fault geometries of well-studied large earthquakes such as Izmit, Kobe, Loma Prieta, Landers, and Hector Mine are constrained largely by surface breaks, geodesy and earthquake seismology. Slip models of such earthquakes are typically based on simplified rectangular planar fault models, oriented parallel to mainshock focal mechanisms and to the general trends of surface breaks (e.g. Izmit: Bürgmann et al., 2002; Kobe: Ide and Takeo, 1997; Loma Prieta: Hartzell et al., 1991; Landers: Freymueller et al., 1994; Hector Mine: Kaverina et al., 2002; Chi-Chi: e.g. Ma et al., 2001). In contrast, the 1999 Chi-Chi thrust-belt earthquake in Taiwan is unusual, because we can independently determine the 3D geometry of the most important faults in considerable detail using techniques and data outlined below. Furthermore the Chi-Chi earthquake is one of the best instrumented large thrust-belt earthquakes (Ma et al., 1999) and thus presents an unusual opportunity to observe coseismic structural growth, comparing coseismic displacements with an independently determined 3D fault model. Finally, significant constraints exist for placing the Chi-Chi earthquake in its larger structural and tectonic setting within the western Taiwan thrust belt.

* Corresponding author. Tel.: +1 609 258 1515; fax: +1 609 258 1274.
E-mail address: lyue@princeton.edu (L.-F. Yue).

0191-8141/$ - see front matter © 2005 Elsevier Ltd. All rights reserved.
doi:10.1016/j.jsg.2005.05.020

2. Basis for Chelungpu–Sanyi fault model

The largest offsets (3–9 m) of the 85-km-long surface break of the Chi-Chi earthquake lie along the northern 50 km segment of the Chelungpu thrust that runs parallel in map view to bedding in the hanging wall in the Pliocene Chinshui Shale (Fig. 1; Lee et al., 2000, 2003). We argue that the Chelungpu thrust must also run parallel to bedding in the subsurface in classic thrust-belt fashion, based on the following evidence: [1] In map view the Chelungpu thrust

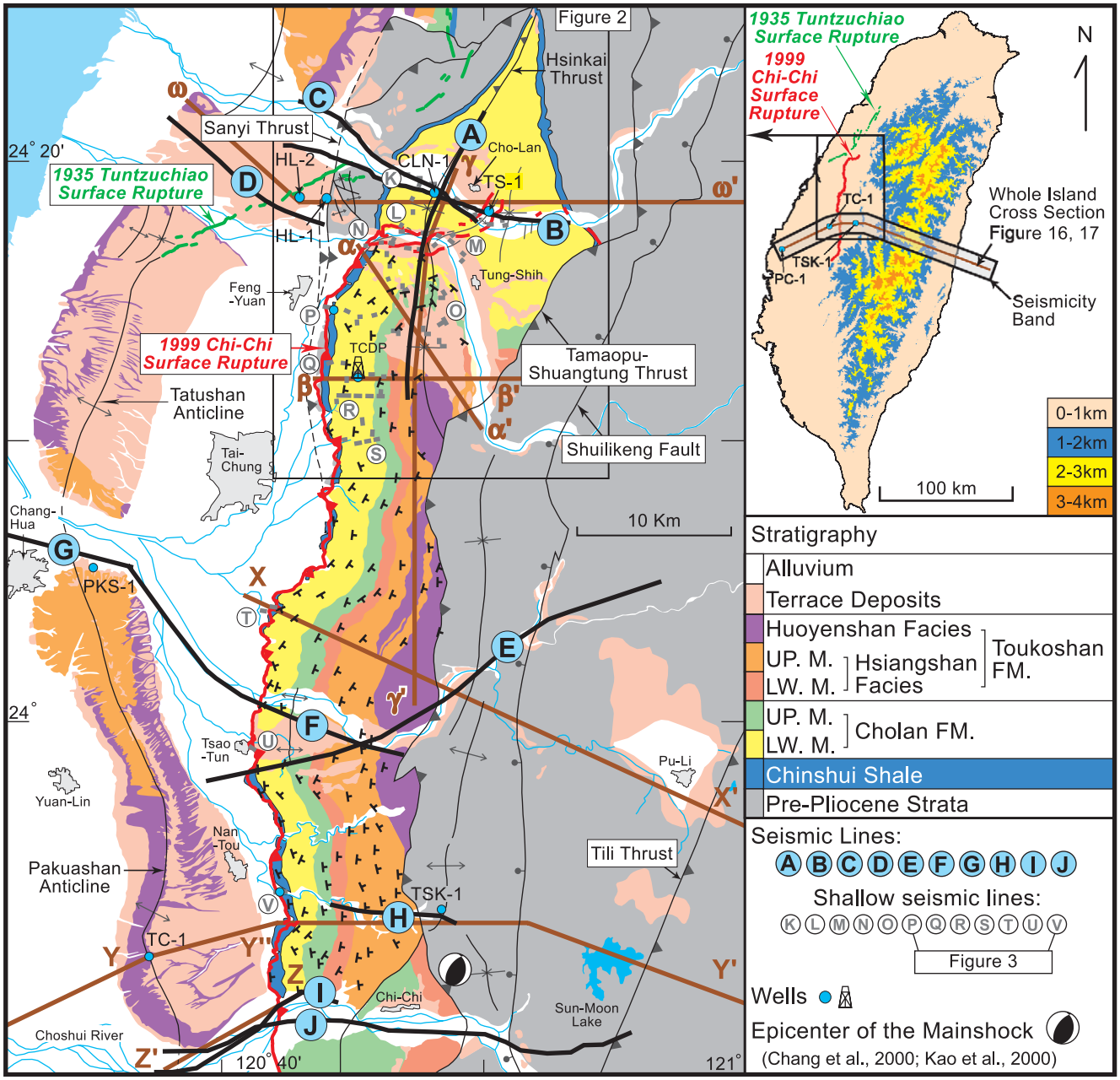

Fig. 1. Geologic map of Chelungpu thrust sheet with the 1999 surface rupture of the Chi-Chi earthquake (M_w=7.6) shown in red (Central Geological Survey, 1999a,b). The trace of the fault runs regionally parallel to hanging wall bedding in the Pliocene Chinshui Shale and to the overlying strata. This parallelism reflects a hanging wall detachment with classic ramp-flat geometry, as shown in cross-sections that are constrained by seismic lines and boreholes. The parallelism between hanging wall bedding and the fault allows us to use surface dip data as a high-resolution constraint on our 3D fault model (Figs. 8 and 9). Geologic maps in Figs. 1 and 2 are compiled from Chinese Petroleum Corporation (1968, 1974, 1982, unpublished), Central Geological Survey (Chang, 1994; Lo et al., 1999; Ho and Chen, 2000; Huang et al., 2000; Lee, 2000) and Chang (1971). Surface breaks of 1935 Tuntzuchiao earthquake (M_L=7.1) in green are from Bonilla (1975). Seismic lines: *A*: Wang (2003); *B*: Hung and Wiltschko (1993); *C* and *D*: Wang et al. (2003); *E*, *F* and *J*: Wang et al. (2002a); *G*: Chen (1978); *H*: Wang et al. (2000); *I*: Hung and Suppe (2002); *K–V*: Wang (2002) and C.Y. Wang et al. (2002a,b,c, 2004). Wells: TS-1, CLN-1, HL-1 and HL-2: Hung and Wiltschko (1993); TSK-1: Suppe (1980); TC-1: Dahlen et al. (1984); PC-1: Lee (1962); TCDP: Taiwan Chelungpu-Fault Drilling Project (in progress).

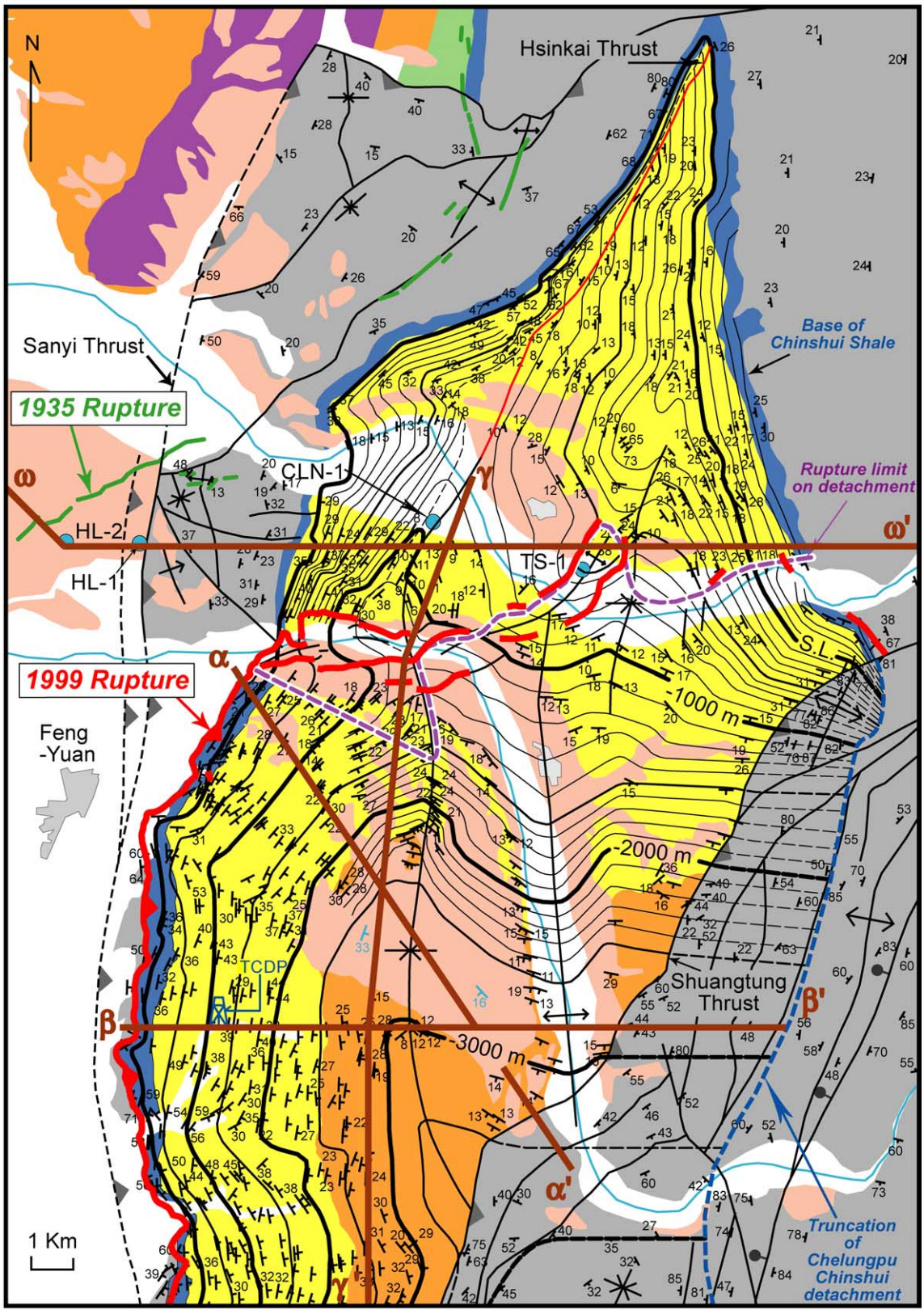

Fig. 2. Geologic map of the northern termination of the 1999 surface rupture (in red). Structure contours on the North Chelungpu Chinshui Shale detachment are shown (100 m interval; see regional map in Fig. 8). The approximate northern limit of rupture on the detachment in the 1999 Chi-Chi earthquake is shown in purple, which is the trajectory of take-off points of forward- or back-thrust ramps and kink-bands connecting to the surface breaks (Hung and Suppe, 2002; J.C. Lee et al., 2002; Y.H. Lee et al., 2003). Contours north of the rupture are on the stratigraphic horizon of the detachment, the bottom of Chinshui Shale. See Fig. 1 for sources.

not only runs parallel to bedding within the immediately adjacent Chinshui Shale, but is consistently parallel to the stratigraphic boundaries of the entire hanging wall, displaying the so-called 'bacon structure' (Fig. 1) typical of maps of classic imbricated thrust belts such as the southern Appalachians and Canadian Rockies in which ramp-flat geometry is well documented (e.g. Roeder et al., 1978; Roeder and Witherspoon, 1978; Mitra, 1988; Price, 2001). The surface break is also generally parallel to the strikes of surface dip measurements in the hanging wall (Figs. 1 and 2). Such parallelism in map view would not be expected if it were not also true at substantial depth and caused by bending of the Chelungpu thrust sheet as it steps up from a detachment in the Chinshui Shale. [2] A number of shallow seismic lines and shallow drilling confirm that the near-surface thrust is parallel to bedding in the upper 500–2000 m; two examples of which are shown in Fig. 3 (Wang, 2002; C.Y. Wang et al., 2002a,b,c, 2004). [3] A number of deep petroleum seismic lines image the Chelungpu thrust and its northern continuation, the Sanyi thrust, to depths of 3–6 km and confirm that it runs parallel to bedding in the hanging wall (for published examples see Hu and Chiu, 1984; Hung and Wiltschko, 1993; C.Y. Wang et al., 2000, 2002a, 2003, 2004).

Based upon these observations that hanging wall bedding is parallel to the fault but footwall bedding is horizontal (Fig. 4B–D), it is a logical necessity that the Chelungpu fault becomes parallel to bedding in the footwall at depth. That is, we are dealing with essentially classic ramp-flat thrust geometry as illustrated schematically in Fig. 4A (Roeder et al., 1978). In particular, the flattening dips in the hanging wall reflect the flattening of the fault to the detachment. Furthermore, the stratigraphic thickness and depth of the detachment horizon in the hanging wall and footwall agree with regional gradients and match at the fault cutoff ($T_h \approx T_f$ in Fig. 4). Fig. 5 shows two line drawings of the seismic reflections parallel to bedding in the hanging wall and flattening to the main Chinshui Shale detachment. A quantitatively very similar cross-section was drawn 15 years prior to the seismic imaging along the same line (Y–Y″–Y′; Figs. 1 and 5) based entirely on extrapolation of the fault downward from the surface, parallel to dip measurements in the hanging wall. This shows that we can effectively predict Chelungpu fault geometry based on the constraint that the fault be parallel to bedding in the hanging wall (fig. 11 in Dahlen et al., 1984; fig. 2-20 in Suppe, 1985).

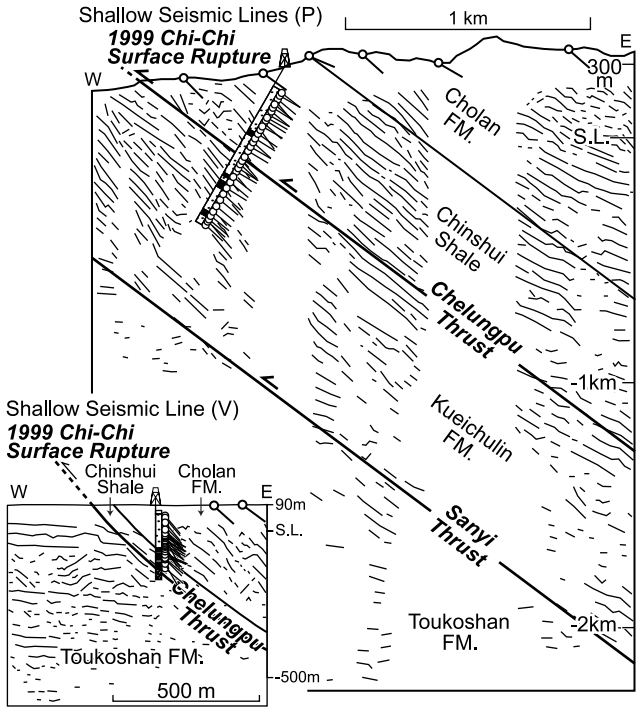

Fig. 3. Line drawings of shallow seismic lines showing parallelism between fault and hanging wall bedding determined from shallow borings and surface dip measurements (Lines *P* and *V* in Fig. 1; Wang et al., 2002a,b,c).

3. Data and methodology

A large number of well-constrained surface dip measurements from published and unpublished geologic maps are the primary data for our extrapolation of the Chelungpu–Sanyi thrust system to depth (Figs. 1 and 2). The density of dip data is illustrated in the map of Fig. 2 and in cross-section $\alpha\alpha'$ of Fig. 6 which also shows the extrapolated fault geometry based on the assumed parallelism of the fault in the Chinshui Shale to the dip of strata measured in the hanging wall. We constructed 47 such cross-sections of the Chelungpu thrust sheet (Fig. 7) based on surface dip data and combined them to form a 3D fault model using a methodology discussed below and in the caption of Fig. 7. Some sections such as those in Fig. 5 had further constraints from seismic lines and wells (lines *A*–*J* in Fig. 1).

We combined our 47 sections (Fig. 7) based on the dip of hanging wall strata to produce a preliminary contour map of the Chelungpu thrust. However, downward extrapolation of the fault in each section based on dip data has cumulative errors that vary from section to section. Random errors of 3° in dip measurement in this case can cause a cumulative vertical error of roughly $\pm$500 m at the base of the ramp at $\sim$5 km depth. Therefore, we corrected the fault contours using the strike data, based on the constraint that fault contours must be everywhere parallel to the strike of associated bedding at the surface. This second step, combined with seismic control, effectively removes much of the cumulative errors associated with the extrapolation of the fault using dip data. The key point is that the strike data are a constraint that is independent from the dip constraint. Furthermore, a set of strike data does not suffer from the same cumulative errors of extrapolation as a set of dip data because strike data are seen as a field in map view; therefore, the strike data interpolation does not lead to cumulative errors.

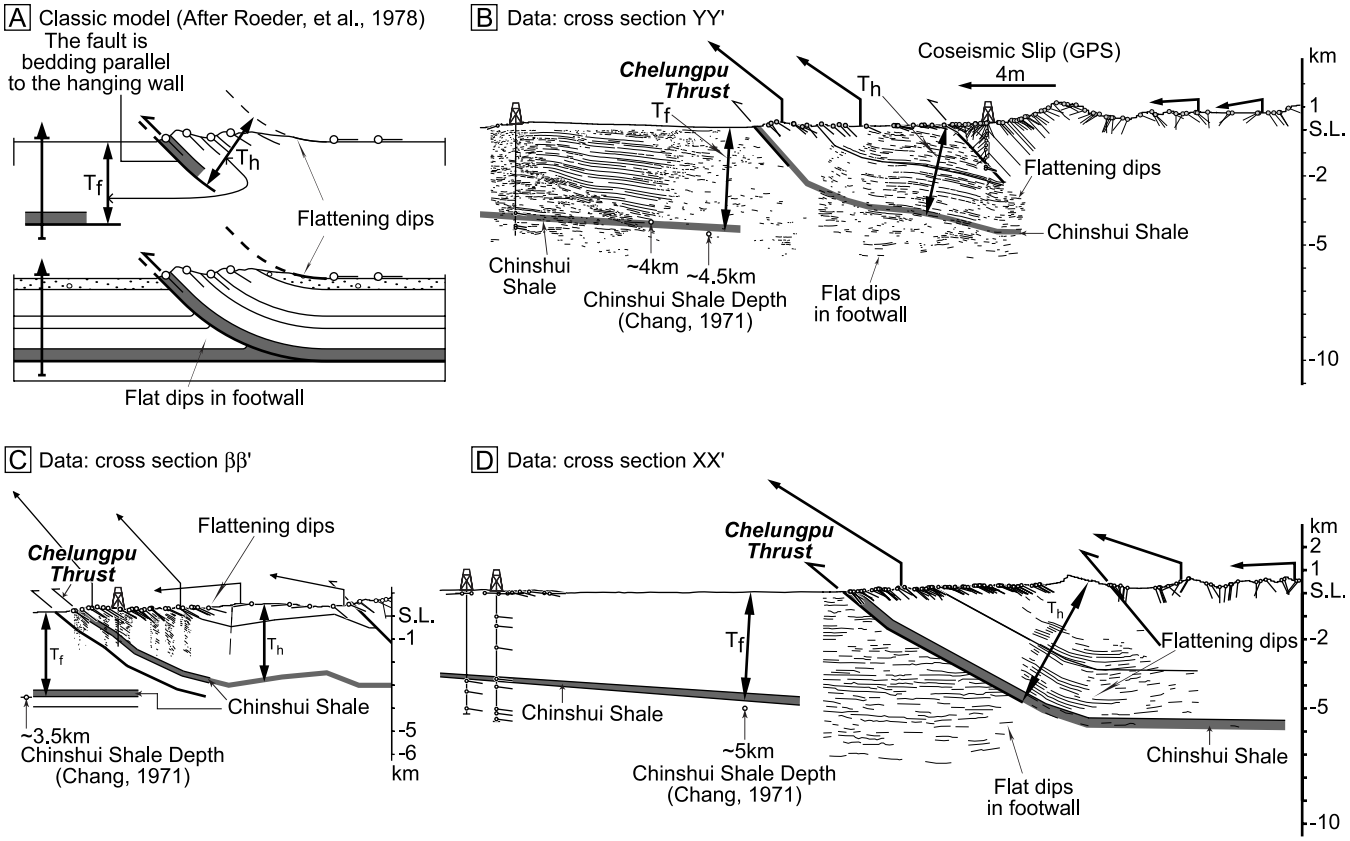

Fig. 4. (A) The classic thrust–ramp model showing that a bedding-parallel fault in the hanging wall logically must flatten to its own stratigraphic level in the footwall (after Roeder et al., 1978). (B)–(D) Data for cross-sections ββ′, XX′ and YY′ of the Chelungpu thrust sheet are analogous to this classic model with the hanging wall running parallel to bedding near the base of the Pliocene Chinshui Shale. Therefore, the Chelungpu thrust ramp must flatten with depth to run along the base of the Chinshui Shale in the footwall. This simple classic concept forms the primary basis for using surface dip data and stratigraphic thicknesses in the hanging wall and footwall to constrain our cross-sections and 3D fault models. The projected coseismic displacement vectors for the Chi-Chi earthquake (Yu et al., 2001) are in general agreement with this classic model (see also Figs. 5 and 14).

The Chelungpu fault model (Figs. 2 and 8) is not constrained by surface dip data east of the Shuangtung thrust because it brings folded pre-Chinshui strata to the surface (Figs. 1 and 2); therefore, fault contours are less certain and are shown as dashed lines (Figs. 2 and 8). Nevertheless, significant general constraints exist in this region of dashed contours. [1] The Chelungpu thrust logically must flatten to a detachment in the footwall within the Pliocene Chinshui Shale because the well-constrained fault lies within the Chinshui Shale in the hanging wall and, therefore, must have a still-existing bedding-parallel footwall segment at depth (Fig. 4A). [2] The location of flattening of the Chelungpu thrust to the Chinshui detachment east of the Shuangtung thrust is constrained by three seismic lines (*E*, *H* and *J*; see Figs. 1 and 5). [3] Furthermore, the base of the fault ramp must lie at the depth of the Chinshui Shale in the footwall ($T_h \approx T_f$ in Fig. 4), which is constrained by published and unpublished seismic lines and wells west of the Chelungpu–Sanyi thrust (e.g. Chang, 1971; Lee et al., 2000). Thus, the Chelungpu thrust may extend not much deeper than the total thickness of the Pliocene and younger strata, which varies from ~3 to 6 km from north to south (Fig. 8). [4] The footwall detachment must have a length not less than the observed length of the matching hanging wall detachment, which is greater than 14 km ($> aa' = bb'$ in Fig. 5, because the hanging wall cutoff of the base of the ramp is eroded).

These constraints substantially limit the range of possible models east of the Shuangtung thrust. In particular, maximum depths to the base of the Chelungpu thrust ramp of greater than 6 ± 0.5 km (5 ± 0.5 km near the Chi-Chi hypocenter) are precluded. This is significant because initial slip in the Chi-Chi earthquake began at a significantly greater depth of 8~10 km, approximately 3–5 km below the Chelungpu thrust, based on refinements of the main-shock hypocenter location shown in Fig. 5 (Chang et al., 2000; Kao et al., 2000). Therefore, slip in the Chi-Chi earthquake did not begin on the Chelungpu thrust, but on a previously unknown fault whose relationship to the Chelungpu thrust we discuss in a later section. However, large slip in the Chi-Chi earthquake is very shallow (~5 km and less) and located on the Chelungpu thrust, judging from geodetic and seismic slip models discussed below and surface breaks (Ma et al., 2000, 2001; Yu et al., 2001; Lee et al., 2003).

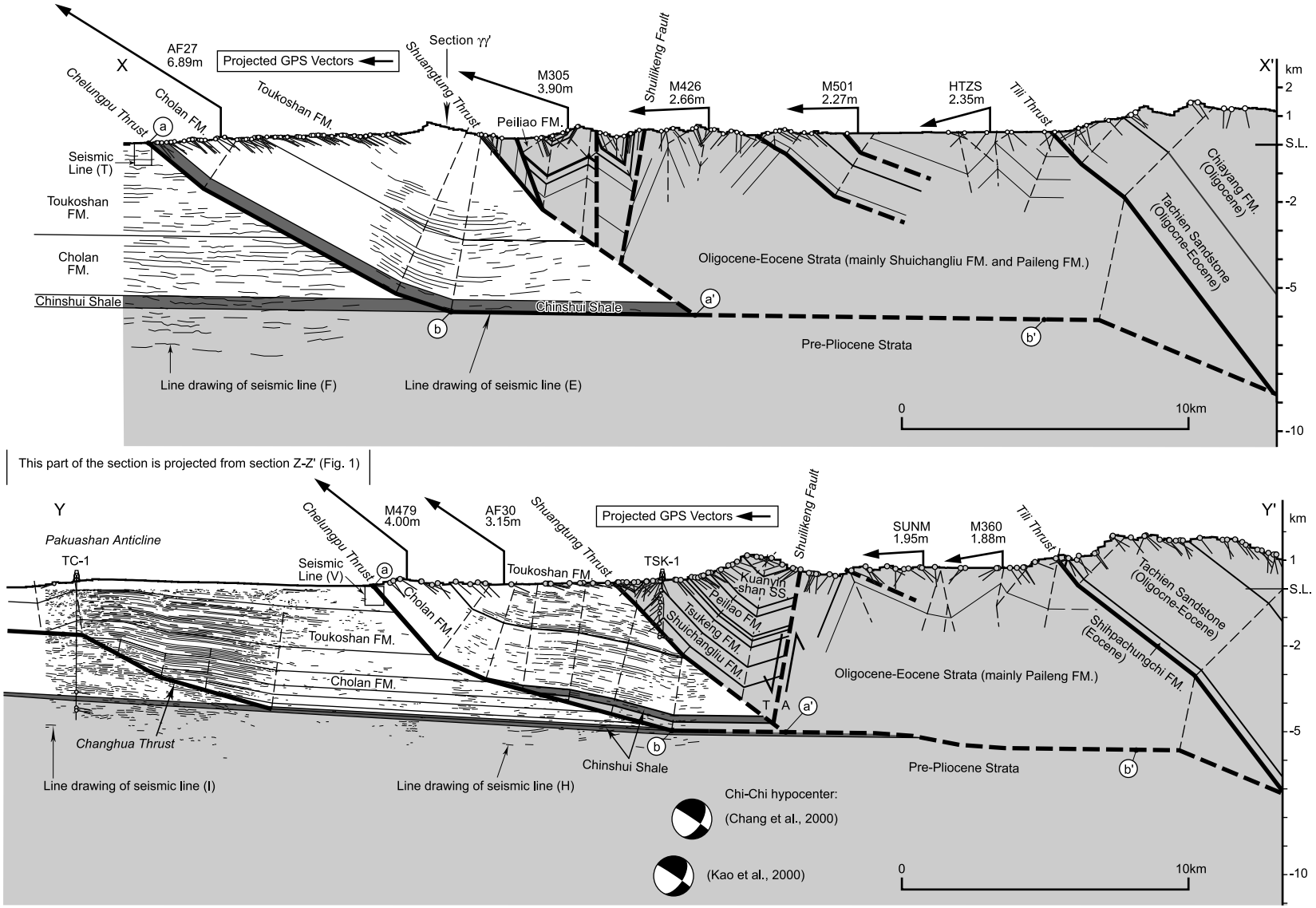

Fig. 5. Regional EW sections XX′ and YY′ with line drawing of reflectors in seismic lines *E*, *F*, *H* and *I* (locations in Fig. 1), showing the Chelungpu thrust flattening to the Chinshui detachment at a depth of 5.5–6 km. The minimum length of the Chinshui detachment must be greater than the preserved length of the hanging wall detachment (at least $bb' = aa'$). The GPS vectors are projected showing the component of coseismic displacement in the plane of the section (station number and total displacement also given; Yu et al., 2001). These vectors are relative to stable Kinmen west of Taiwan, but they also approximately show the displacement of the Chelungpu hanging wall relative to the footwall because displacements of the footwall relative to Kinmen are very small (Fig. 8). Note that the vectors are approximately fault parallel suggesting that the surface coseismic displacement is dominated by net structural growth (see also Fig. 14). For Pakuashan anticline also see the caption of Fig. 16.

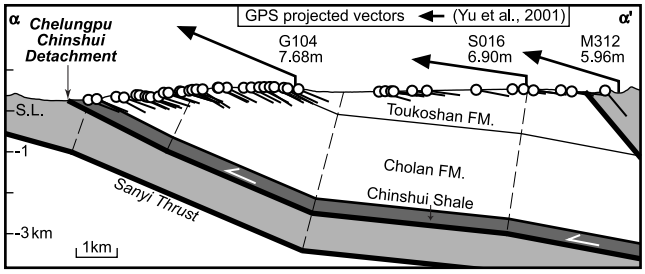

Fig. 6. In cross-section ($\alpha\alpha'$, location in Fig. 1) the dip of the fault model is constrained to be parallel to surface dip measurements, following the classic thrust–ramp model (Fig. 4A). Note that the coseismic displacement vectors from GPS (Yu et al., 2001) are also approximately parallel to the bedding dips and fault model (see text).

4. New Chelungpu–Sanyi fault model

The new 3D model of the Chelungpu–Sanyi thrust system (Figs. 8 and 9) displays an essentially classic ramp-flat geometry, but with the added complexity of branching northward into two faults along a branch line that is shown in the models. There are thus three major fault segments to consider, only two of which produced surface rupture in the Chi-Chi earthquake: [1] south of the branch line the main Chelungpu thrust steps up from the Pliocene Chinshui Shale detachment, [2] north of the branch line this main thrust is possibly inactive and is called the Sanyi thrust, which steps up from stratigraphically deeper Pliocene and Miocene detachments in the Kueichulin and Tungkeng/Kuanyinshan Formations, and [3] north of the branch line the North Chelungpu Chinshui detachment is a relatively new bedding-parallel fault in the Chinshui Shale that feeds slip off of the main Sanyi–Chelungpu thrust and is the locus of some of the largest displacements in the Chi-Chi earthquake. North of the branch line the Sanyi thrust and North Chelungpu detachment are in many places parallel faults as shown in several cross-sections (Figs. 5, 6, 10 and 11), thus the shape of the North Chelungpu detachment to a considerable degree reflects the shape of the underlying Sanyi thrust.

The intersection of the branch line with the land surface is straightforwardly marked by the point at which surface rupture departs northward from the main Sanyi–Chelungpu thrust to run along the North Chelungpu detachment in the Chinshui Shale; this point is therefore the southernmost limit of Kueichulin Formation in the hanging wall (Figs. 1 and 11). This same branch point is seen in N–S section $\gamma\gamma'$, which is drawn within the Sanyi ramp (Fig. 11).

There is a strong N–S variation in depth to the base of the east-dipping Sanyi–Chelungpu ramp at the level of the Chinshui Shale (1–6 km) and in the elevation of the Chinshui Shale and Kuanyinshan detachments (~4–6 km). There is thus an E–W-trending trough-shaped structure to the detachment at the Chinshui level, here called the Tsaotun trough, which reflects a strong primary N–S variation of the thickness of the Chinshui Shale and younger stratigraphic section, as seen in the

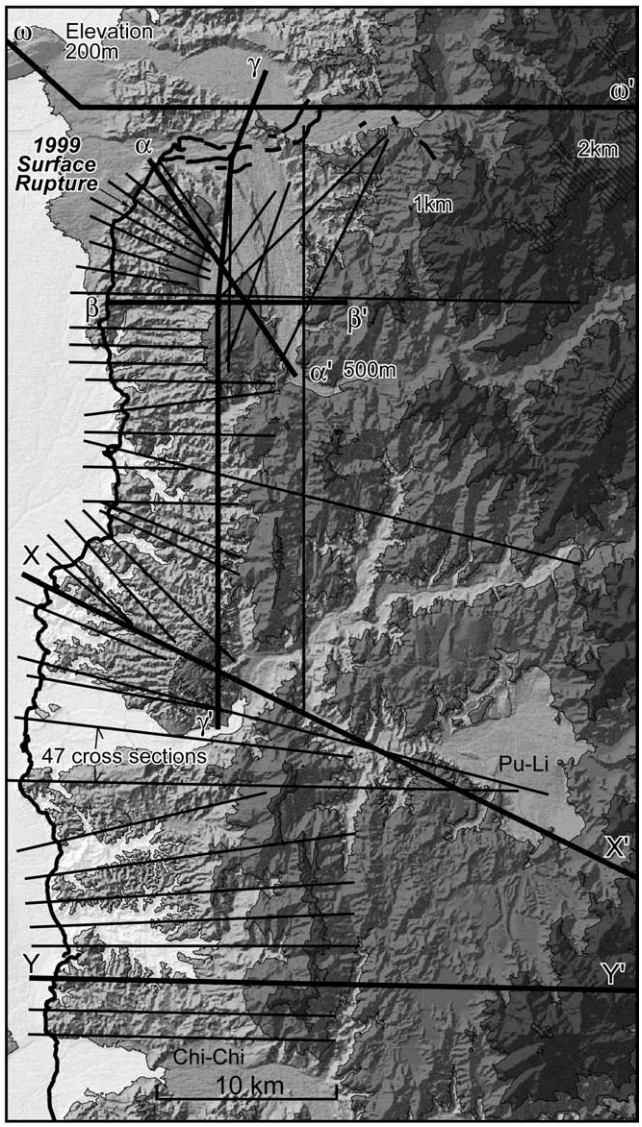

Fig. 7. Topographic map with locations of 47 cross-sections for constructing the 3D Chelungpu fault model. We constructed each cross-section by extrapolating the fault downward parallel to surface dip data gathered from geologic maps (Fig. 1). See Figs. 4–6 for examples. We combined those cross-sections to make the 3D fault model (Fig. 8) using the constraint that the strike of the contours be parallel to the strike of associated bedding in the hanging wall.

Taichung basin west of the Chelungpu thrust (Chang, 1971; Lee et al., 2000 and Fig. 8).

The dip of the Sanyi–Chelungpu ramp is not constant, but is typically ~40–55° near the surface and rather abruptly changes to ~15–25° at ~3 km depth, especially in the south (see Fig. 5). The ramp itself shows large-scale (~5 km) corrugations that are reflected in the Chi-Chi surface breaks and quasi-conformable dip data in the hanging wall (Fig. 1).

Near the northern termination of the Chi-Chi surface break the rupture turns abruptly to the east at Feng-Yuan, departing from the Chinshui Shale detachment to form a complex system of surface faults and folds in younger strata

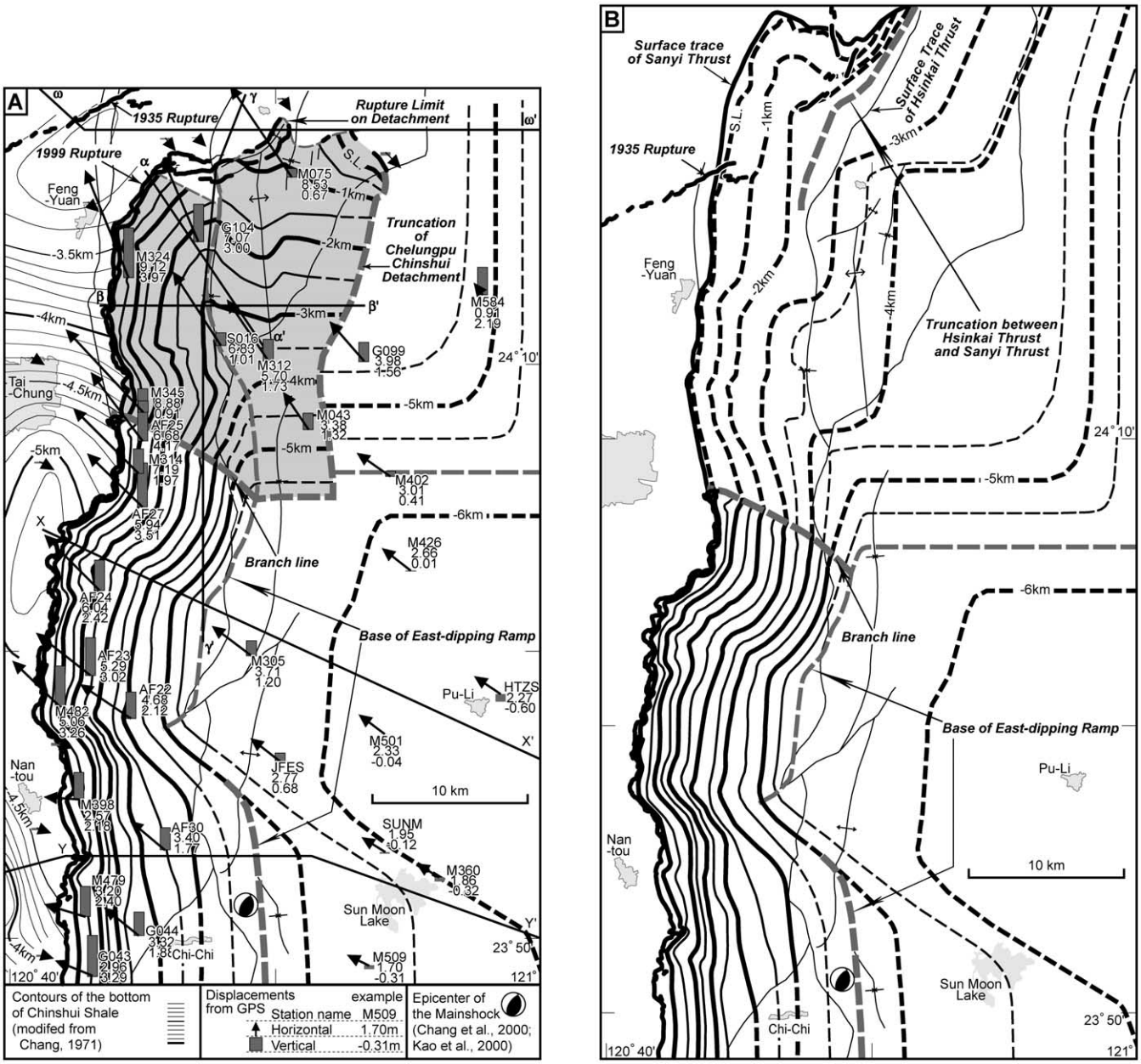

Fig. 8. (A) Chelungpu fault model (500 m contours) together with the horizontal and vertical components of the GPS coseismic displacements of Yu et al. (2001). The geometry of the fault ramp is constrained in detail where the contours are solid, showing large-scale (~5 km) corrugations that are also seen in the surface rupture and in hanging wall folding (see Fig. 1). The Chinshui Shale detachment east of the base of the ramp shows an E–W trough-like structure that reflects the primary shape of the Tai-Chung basin, also shown in the contours of the depth to the Chinshui Shale west of the Chelungpu thrust (Chang, 1971). The depth to the Chinshui detachment reaches a maximum of about 6 km in the trough. East of the Shuangtung fault where the contours are dashed the model is not constrained by surface dips but is still significantly constrained in general (see text). The North Chelungpu Chinshui Shale detachment, shown in gray, takes off northward from the Sanyi–Chelungpu thrust along the branch line (see 3D fault model in Fig. 9 and sections ββ′ and γγ′ in Figs. 10 and 11). The North Chelungpu Chinshui Shale detachment is truncated to the east by the Shuangtung thrust, which raises questions about where slip on this fault roots. B. Sanyi fault model (1000 m contours) is constrained by three cross-sections based on seismic lines and wells (ββ′, γγ′ and ωω′) and local sections based on surface dips. South of the branch line the Sanyi thrust and North Chelungpu Chinshui Shale detachment merge to become a single Sanyi–Chelungpu thrust.

(Figs. 1 and 2). This E–W zone of surface deformation cuts across the south-plunging Cholan syncline and finally rejoins the Chinshui Shale at the surface in the easternmost mapped surface breaks (Fig. 2). This E–W zone of deformation shows a large component of N–S compression on complex forward and back thrusts (Hung and Suppe, 2002; J.C. Lee et al., 2002; Y.H. Lee et al., 2003). This zone is broadly located above an E–W kink band produced by the Feng-Yuan hanging wall transverse ramp in the Sanyi thrust caused in a change in detachment level between the Kueichulin and Tungkeng/Kuanyinshan Formations (see Fig. 11). Our best estimate of the northern limit of slip

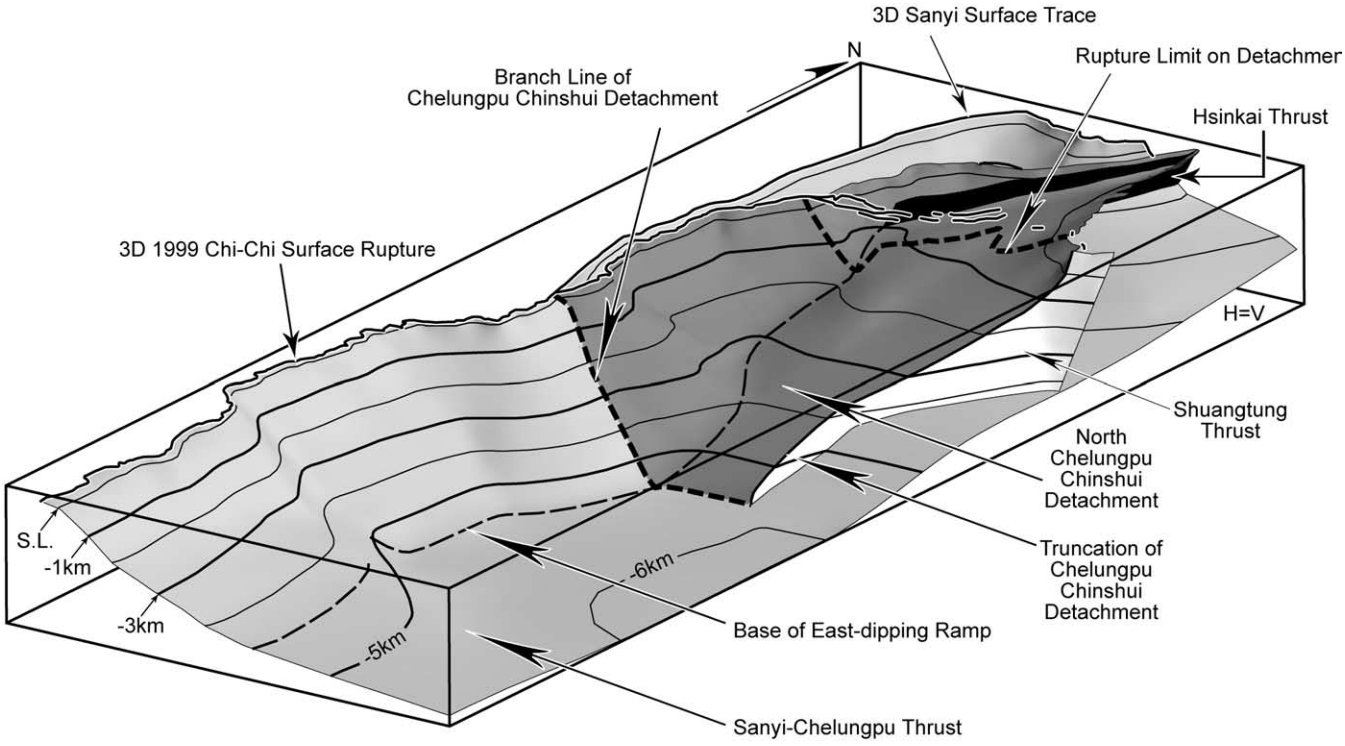

Fig. 9. Oblique 3D view of Sanyi–Chelungpu fault model (Fig. 8), showing its ramp-flat geometry and the E–W trough shape of Chinshui Shale detachment east of the base of the ramp. The North Chelungpu Chinshui Shale detachment branches northward from the Sanyi–Chelungpu thrust. The North Chelungpu detachment is truncated to the east by the Shuangtung thrust, which raises questions about how slip is fed into this detachment.

during the Chi-Chi earthquake on the Chinshui Shale detachment, below this E–W zone, is shown in Figs. 2, 8 and 9.

The eastern limit of slip on the North Chelungpu Chinshui Shale detachment is less straightforward and structurally complex. In map view, we see that the Chinshui Shale is cut off by the Shuangtung thrust at the surface at the easternmost limit of mapped surface rupture, just south of section $\omega\omega'$ (Fig. 2). The subsurface continuation of this cutoff line is shown on the contour maps of Figs. 2 and 8. South of the main Chelungpu branch line the Shuangtung thrust flattens to the Chelungpu Chinshui Shale detachment (Fig. 5). North of the branch line the Shuangtung thrust is interpreted to flatten to the same Sanyi–Chelungpu detachment system, which in Fig. 10 runs in the Kueichulin Formation. Thus, the North Chelungpu Chinshui detachment is everywhere cut off to the east by the Shuangtung thrust. This raises a significant issue of how slip is fed into this detachment at the Chinshui Shale level.

A possible resolution to this issue of truncation is found in the south-plunging Tungshih anticline within the larger Cholan syncline, which folds the North Chelungpu Chinshui detachment (Figs. 2 and 10). The Tungshih anticline may serve to transfer slip from the Sanyi Kueichulin detachment to the shallower North Chelungpu Chinshui detachment, as shown in Fig. 10 and discussed further later.

5. Comparison of Chelungpu fault model with coseismic displacement magnitudes

We are now in a position to compare our 3D Chelungpu fault model with independent constraints on displacement in the Chi-Chi earthquake. We adopt the strategy of initially comparing the 3D fault geometry (Figs. 2, 8 and 9) with coseismic displacements at the land surface (Fig. 12) rather than with coseismic slip on the fault surface based on modeling of geodetic or seismic data, because the observed land surface displacement field has much higher spatial resolution, lower uncertainty and is independent of assumed or computed simplified fault geometries of the slip models. Furthermore, the Chelungpu fault is everywhere within 5–6 km of the land surface because of the shallow detachment. Nevertheless, models of net coseismic slip on the fault are qualitatively similar to the observed land surface displacements in both orientation and magnitude (e.g. Ma et al., 2000, 2001; Ji et al., 2001, 2003; Johnson et al., 2001; Loevenbruck et al., 2001, 2004; Sekiguchi and Iwata, 2001; Wu et al., 2001; Zeng and Chen, 2001; Dominguez et al., 2003; Johnson and Segall, 2003; W.M. Wang et al., 2004). Later, we compare the 3D fault model with models of the Chi-Chi slip history of Ma et al. (2001) and Ji et al. (2003) and with a geodetic inversion for fault geometry of Johnson and Segall (2003).

Coseismic surface displacement data come primarily from two observational sources: [1] ground-based GPS

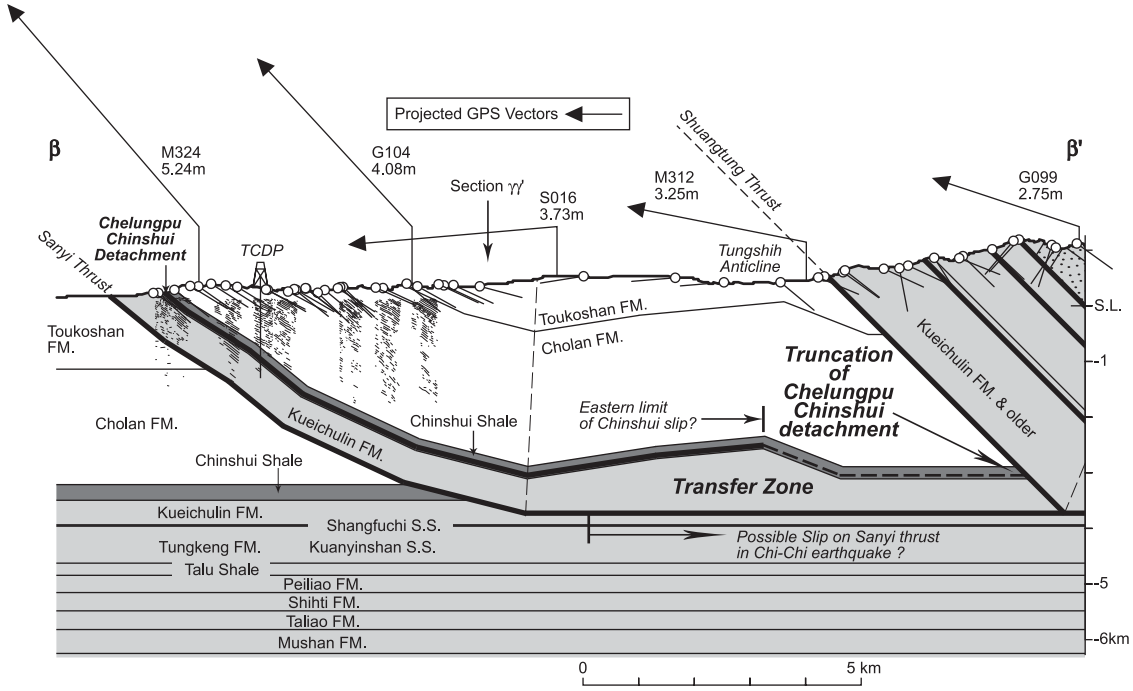

Fig. 10. EW cross-section ββ′ passing through the Taiwan Chelungpu Drilling Project deep scientific borehole (TCDP) with line drawing of seismic reflectors in seismic line Q (location in Fig. 1), showing the eastward truncation of the North Chelungpu Chinshui detachment by the Shuangtung thrust. This eastward truncation of the Chinshui Shale, which is also seen on the surface geologic map just south of section ωω′ (Figs. 1 and 2), raises questions of where slip on this detachment roots. Here, we suggest that the Tungshih anticline transfers slip between the Chinshui detachment and the Sanyi Kueichulin detachment, either as a detachment fold or duplex zone. Thickening in the Tungshih anticline at the Kueichulin level is seen in seismic line *B* to the north (Fig. 18, section ωω′). Note that the coseismic surface displacements from GPS (Yu et al., 2001) are approximately parallel to the fault at depth. Due to the oblique orientation of the section with respect to the coseismic displacement (Fig. 8), the GPS vectors were corrected for the N–S regional plunge of the Chinshui detachment (see Fig. 8; this preserves the component of displacement in the plane of the section, without generating artifacts from uplift associated with the N component of displacement).

geodetic displacements computed relative to Kinmen Island ~200 km west of Taiwan (Fig. 12B; Yu et al., 2001) and [2] satellite photogrammetry based on parallax measurements between high-resolution *Spot* images taken before and after the Chi-Chi earthquake (Dominguez et al., 2003). Excellent data on surface ruptures exist, but the slip vectors are locally complex and heterogeneous because of a variety of near-surface phenomena unrelated to the deep fault geometry (Lee et al., 2003). The photogrammetric (*Spot*) displacement field enfolds the GPS data as control and is remarkable in that it gives a continuous image of horizontal displacements with high spatial resolution (Fig. 12A and C). We compare these two coseismic surface displacement fields with our new fault model, first focusing on the displacement magnitudes and then their orientations.

The most striking first-order comparison between the fault model and the horizontal component of the surface displacements is that the areas of large displacement lie almost entirely above the Sanyi–Chelungpu ramp north of the Tsaotun trough (north of segment *h*; Fig. 12D) and above the Feng-Yuan transverse ramp and west of the crest of the Tungshih anticline at the northern termination (segments *a–d*; Fig. 12D). Furthermore, large vertical components (Fig. 8) and large surface breaks are all in this region (Yu et al., 2001; Lee et al., 2003). Smaller, but still significant (1–3.5 m) displacements are recorded above the ramp south of the Tsaotun trough and above the detachment. Thus, without actually modeling the coseismic displacements on the fault surface, the high-resolution coseismic surface data (Fig. 12) suggest a strong segmentation of slip into ramp and flat geometric segments (Dominguez et al., 2003).

At a finer scale, a number of details of the high-resolution *Spot* displacement–magnitude map (Fig. 12C) correlates with the details of the fault model. [1] Most obvious is the high-displacement patch centered over the boundary between ramp facets labeled *g* and *h* in Fig. 12D. [2] The next facet to the north (N–S striking segment *f*) also appears as a distinct segment in the displacement map with an abrupt increase in displacement northward coinciding with the NE-trending segment *e*, which is the major branch line marking the beginning of the North Chelungpu Chinshui detachment. [3] There is an abrupt reduction of displacement southward at the south edge of ramp facet *i*. [4] A less abrupt change in displacement magnitude marks the boundary between ramp facets *b* and *c*. Some significant segment boundaries in the displacement field are at a high angle to the slip vectors (e.g. the base of the ramp and the crest of the Tungshih anticline), whereas others are approximately parallel to the slip vectors (ramp facet *i* and facet boundary *g–f*, see also the next section). From these observations of displacement segmentation in relation to fault geometry we can infer very

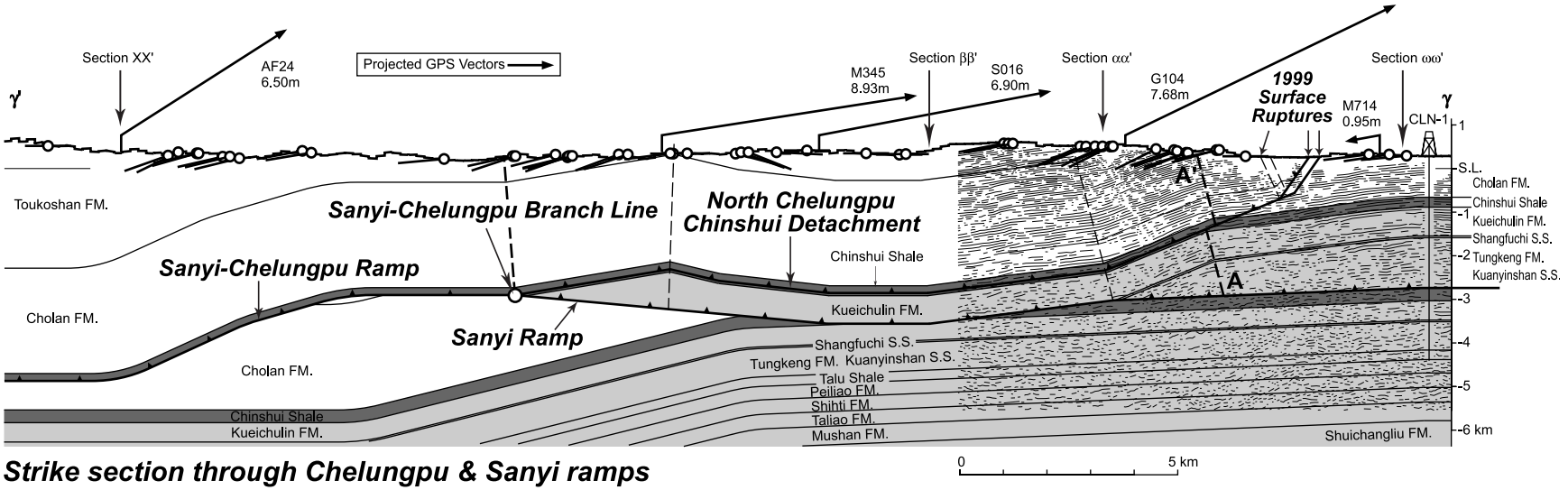

Fig. 11. Regional NS section $\gamma\gamma'$ passing through the EW-trending surface rupture at the northern limit of the Chi-Chi earthquake. The section is constrained by seismic lines *A* (line tracings of reflectors shown in this figure), well CLN-1, surface mapping and E–W sections. This is a strike section passing through the Sanyi–Chelungpu ramp (see dip sections XX′, $\alpha\alpha'$, $\beta\beta'$ and $\omega\omega'$; Figs. 5, 6, 10 and 18). The section shows the North Chelungpu Chinshui detachment stepping up northward from the Sanyi–Chelungpu thrust at the Sanyi–Chelungpu branch line. From the offset of the axial surface A and A′ the total slip on the North Chelungpu detachment is only about ∼0.3 km, indicating that it is a relatively new fault that has slipped only about ∼35 Chi-Chi events in contrast with the Sanyi–Chelungpu fault which has slipped >14 km. GPS coseismic displacement vectors are approximately parallel to the fault and show a large northward strike component to the Chi-Chi displacement (vectors projected similar to Fig. 10).

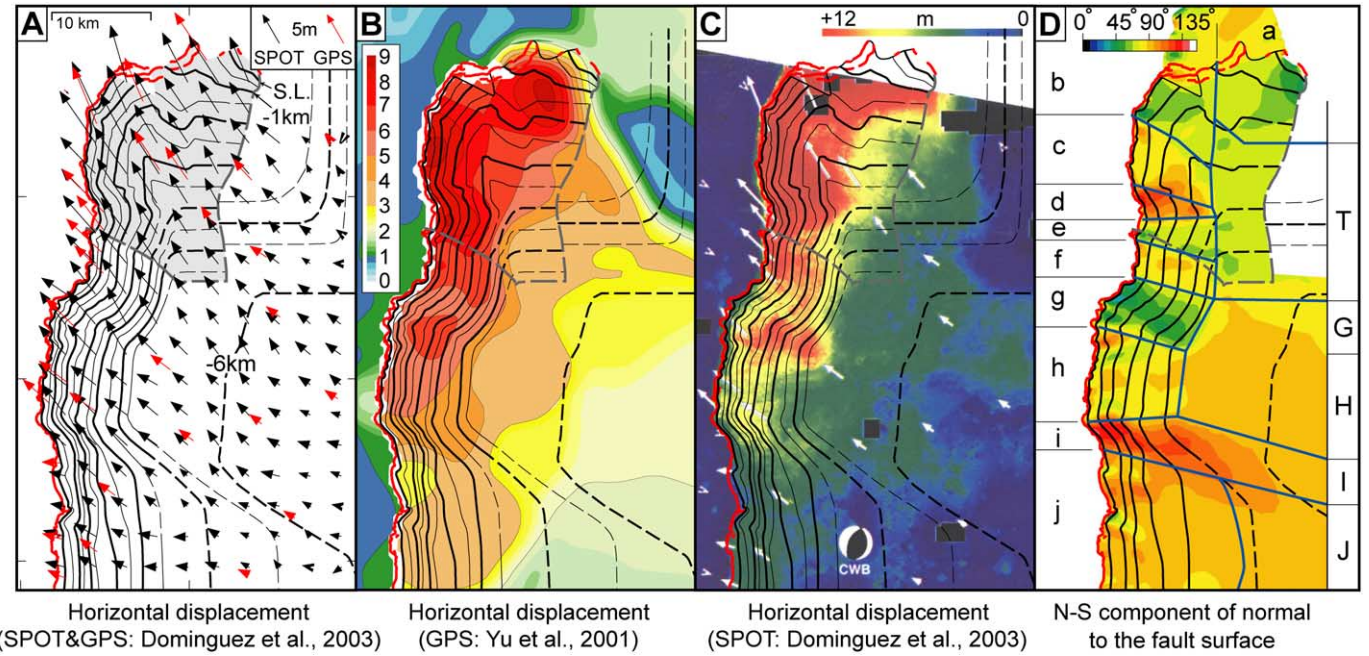

Fig. 12. Map-view comparison between the Chelungpu fault model (Fig. 8A) and 1999 coseismic surface displacements of the Chi-Chi earthquake from GPS and *Spot* (Yu et al., 2001; Dominguez et al., 2003). Large displacement magnitudes (>6 m) are closely correlated with the northern ramp and northernmost transverse ramp. In contrast, the Chinshui detachment and southern ramp show lower displacement magnitudes (<5–6 m). The geometric segmentation of the ramp is visualized in (D) using the NS component of the fault normal, allowing differences in strike to be seen; segments are labeled *a*–*j*. Comparing with the *Spot* high-resolution displacement–magnitude map (C) we see slip closely associated with specific ramp segments or segment boundaries, such as *g* and *a*–*e* and low slip with others, such as *h* and *j*. Significant surface displacement extends about 6–10 km east of the eastern truncation of the North Chelungpu detachment, which suggests that slip to the east may have been on the Sanyi thrust or a deeper fault (see Fig. 10).

substantial geometric segmentation of fault slip at the observable scales in the Chi-Chi earthquake.

Johnson and Segall (2003) have inverted the coseismic GPS observations for a best-fitting fault geometry composed of four planar fault segments. Their best-fitting model is composed of a NS ramp dipping 26°, a detachment dipping 0° at a depth of 5.8–8.6 km, an EW transverse ramp at the northern end dipping 23°, and a small fault segment transitional between the two principal ramps. In light of the difficulties of geodetic inversions, the Johnson and Segall model is in remarkable agreement with our geologically constrained fault model. In our fault model, the NS ramp can be approximated as dipping 32°, which is the average dip of all bedding measurements on the ramp, and the EW transverse ramp at the northern end can be approximated as dipping 15° (at the depth between 0 and 1 km the average dip is 24° and at the depth between 1 and 5.5 km the average dip is 13°). As such it provides some support for the more fine-grained comparison given above using the high-resolution surface displacement field of Dominguez et al. (2003) and our higher-resolution fault model.

Johnson and Segall (2003) also propose that slip in the Chelungpu Chinshui detachment during this earthquake should extend to the east about 27 km from Feng-Yuan based on their inversion results. However, the Chelungpu Chinshui detachment does not extend more than 16 km to the east because it is truncated by the Shuangtung thrust. A plausible interpretation is that the eastern Sanyi detachment might have slipped during the earthquake and slip was transferred through the Kueichulin Formation to the North Chelungpu Chinshui detachment through growth of the Tungshih anticline (Fig. 10). This idea seems supported by similar measurements between the GPS coseismic vertical displacement and structural coseismic uplift around the Tungshih anticline. The difference of the GPS coseismic vertical displacement between GPS stations M312 and S016 is about 0.70∼0.95 m, depending on the method projecting stations onto cross-sections (Figs. 6 and 10). With a 6∼9-km-wide, 700∼900-m-thick transfer zone and a 3 m fault slip, the structural coseismic uplift (height, from regional bedding to the highest peak of a triangular-shape uplift profile; Figs. 6 and 10) is about 0.60∼0.75 m.

Post-seismic GPS displacements in the first 3–15 months have also been inverted for the dip and depth of a detachment (Hsu et al., 2002; Yu et al., 2003). They also arrive at a best-fitting detachment dip of 0°, but the best fitting depth is 10–12 km, which is substantially deeper than the Chelungpu fault, possibly suggesting accelerated creep on the Taiwan Main detachment (Hsu et al., 2002; Yu et al., 2003). However, it should be noted that on a longer timescale, the post-seismic GPS observations and after-shock sequences might be actually dominated by a combination of deep afterslip on the deep ramp and Main detachment (Perfettini and Avouac, 2004), and also broader scale viscous deformation.

6. Comparison with models of Chi-Chi slip history

Several models of the spatial and temporal distribution of slip over the ∼30 s duration of the Chi-Chi earthquake have been inverted from teleseismic, strong motion and GPS data (Ma et al., 2000, 2001; Ji et al., 2001, 2003; Sekiguchi and Iwata, 2001; Wu et al., 2001; Zeng and Chen, 2001; W.M. Wang et al., 2004). The planar fault models used in these inversions are in effect ramp models because they contain no flat detachment, being based largely on the mainshock focal mechanism and general strike of the surface rupture. The model fault is typically a ∼30° east-dipping plane but some inversions used 2–4-segment fault models based on the shape of the surface rupture. As a group these models agree best among themselves within the regions that closely approximate the actual fault ramp as located by our 3D fault model, in contrast with the regions of the detachment and northern transverse ramp where there is strong disagreement among the slip models.

Here, we compare our 3D fault model with the slip history of Ma et al. (2001) because it has relatively high spatial and temporal resolution. We also make some comparisons with the more complex slip model of Ji et al. (2003), which does the best job of modeling waveforms.

The two-segment fault model of Ma et al. (2001) is based on teleseismic and strong-motion data and is composed of one 29° east-dipping ramp and one 29° south-dipping subramp (the average dip of all bedding measurements on the east-dipping ramp is 32°). Thus this model only closely approximates our 3D fault model within the vicinity of the NS-striking Chelungpu fault ramp, as is seen from the 3D view in Fig. 13. The main body of Fig. 13 is a set of maps showing a vertical projection of Ma's slip model onto our 3D fault model for each of 27 one-second time steps. In general, we see close relationships between details of the Ma's slip model (Fig. 13) and the main geometric fault segments (identified in Fig. 12D). What emerges from this comparison is a pattern of slip being temporally confined to specific fault segments for as long as 10 s with a stagnation or retardation of rupture propagation at some geometric segment boundaries.

The spatial–temporal patterns of slip history can be generalized as follows. [1] Three seconds elapsed before finite slip emerges in the model, which is roughly the time required for rupture to propagate at a typical velocity of

Fig. 13. Map-view comparison between the Chelungpu fault model and Chi-Chi fault-slip history, based on seismology from Ma et al. (2001) and Ji et al. (2003). Note in the 3D views that the simplified fault models used for the slip-history inversions (shown in pink) only approximate the Chelungpu fault model (shown in gray) in the vicinity of the fault ramp. These inversions contain no detachment. A number of close correspondences exist between details of the slip and details of the 3D fault model, as discussed in the text. For example, adjacent geometric ramp segments *b–d* show patches of very different slip in the total-slip model of Ji et al. (2003), which suggests that total fault displacement cannot simply be the sum of identical Chi-Chi events. The slip models are projected vertically.

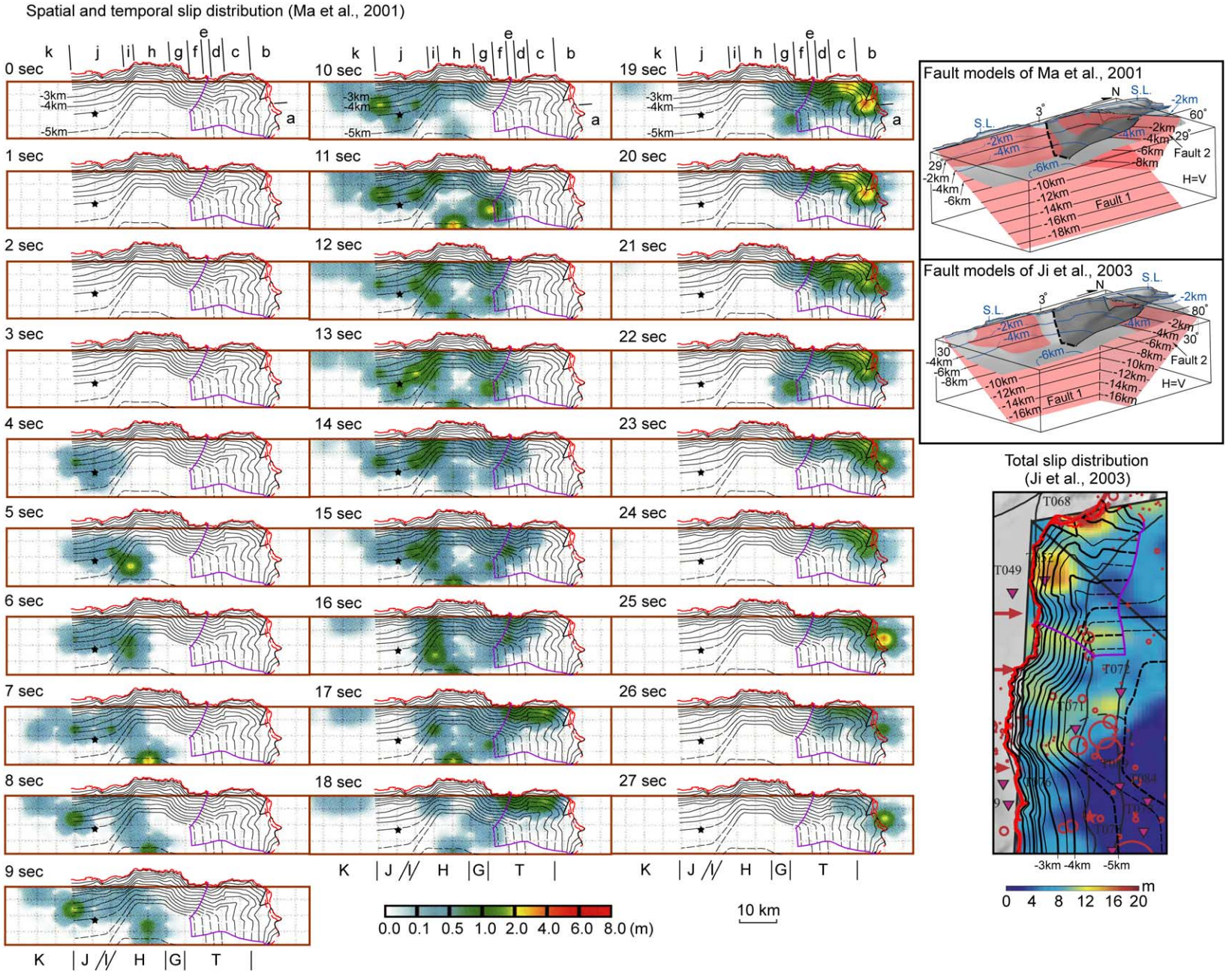
Spatial and temporal slip distribution (Ma et al., 2001)
k j i h g f d c b e a
0 sec
1 sec
2 sec
3 sec
4 sec
5 sec
6 sec
7 sec
8 sec
9 sec
10 sec
11 sec
12 sec
13 sec
14 sec
15 sec
16 sec
17 sec
18 sec
19 sec
20 sec
21 sec
22 sec
23 sec
24 sec
25 sec
26 sec
27 sec
-3km
-4km
-5km
K J I H G T
0.0 0.1 0.5 1.0 2.0 4.0 6.0 8.0 (m)
10 km
Fault models of Ma et al., 2001
Fault models of Ji et al., 2003
N
S.L.
Fault 1
Fault 2
H=V
Total slip distribution
(Ji et al., 2003)
T068
T049
T071
T076
T084
-3km -4km -5km
m
0 4 8 12 16 20

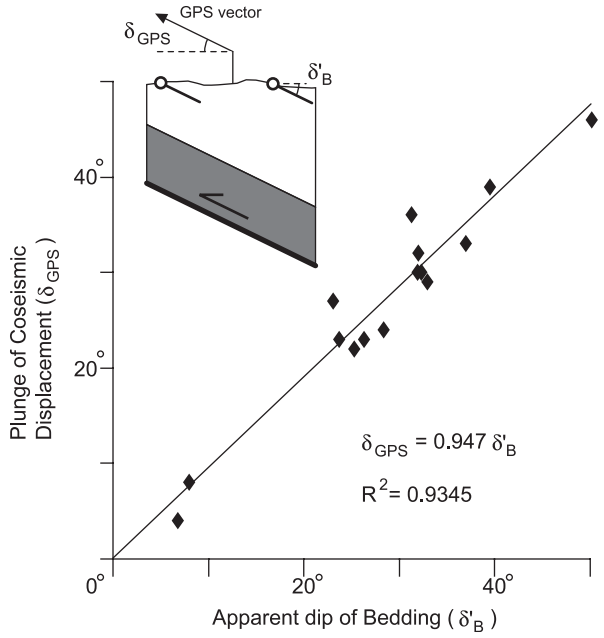

Fig. 14. Parallelism of local orientation of bedding above the Chelungpu ramp and coseismic surface displacements of the 1999 Chi-Chi earthquake. The plunges of GPS coseismic displacements δ_{GPS} (Yu et al., 2001) are parallel to local bedding (apparent dip of bedding in the GPS azimuth δ'_B) with good statistics. This shows that the coseismic displacements are dominantly fault parallel and largely reflect net structural and geomorphic growth. Data from ramp segments *b–j* of Fig. 12D. This parallelism is also seen in GPS vectors projected onto the cross-sections of this paper.

∼2 km/s from the hypocenter at ∼8–10 km depth to the Chelungpu fault (cf. Ji et al., 2003). [2] Finite slip first emerges at 4 s in the southern ramp segment *j* and continues until 15 s. No slip is seen in the flat *J* to the east, in qualitative agreement with smaller surface geodetic displacement in this region (Fig. 12C). [3] Slip is retarded from propagating into ramp segments *h* and *g* until 10–11 s. [4] Slip also is retarded at the northern end of segment *g* from 11 to 14 s after which it propagates steadily northward along the ramp and into the northern transverse ramp. The slip model shows high-resolution agreement with the location of the northern ramp in our 3D fault model, suggesting again that large slip is largely confined to the Chelungpu ramp. It should be noted that nearly no slip is seen in the northern transverse ramp except at its western end at 19 and 26 s, which is where larger surface displacement is seen in the geodetic data (Fig. 12B and C). The slip model of Ji et al. (2003) shows major slip extending much farther eastward in their northern transverse ramp where Johnson and Segall (2003) argue for some slip extending 27 km to the east (see discussion above). [5] The only area of substantial slip that projects into the area of the Chelungpu detachment from Ma's model is in the central segments *G*, *H* and *I* where slip emerges at 5 s and continues to 19 s. This is in qualitative agreement with relatively large geodetic surface displacements above these segments (Fig. 12B and C) even though the fault model of Ma et al. (2001) contains no detachment. [6] Transverse ramp segments *i–I* show a pattern of long-continued activity with bursts of radiation between 5 and 17 s, which suggests that these zones are significantly more complex than shown in our 3D fault model. Transverse ramp segments *g–G* show a similar pattern on long slip with bursts of radiation between 11 and 22 s.

The slip model of Ji et al. (2003) shows similar features in the ramp to the model of Ma et al. (2001), but does the best job to date of fitting waveforms, which may imply a better spatial resolution. High-resolution is also suggested by close correlations with our 3D fault model. In particular Ji's model shows two localized high-slip patches (∼12 m) in the northern ramp; these coincide with our ramp patches *c* and *f* (or the branch line), with the intervening patches showing lower slip. Ji's model also shows large slip (∼10 m) localized along the juncture between ramp segments *g* & *h* and *h* & *i*.

In general these correlations between the details of the 3D fault geometry and the seismologic models of slip history confirm a strong control of geometric segmentation on slip history in the Chi-Chi earthquake. Significant segment boundaries exist transverse to both the slip and propagation directions.

7. Comparison with coseismic displacement orientations

The orientations of the geodetic displacement vectors are closely related to the fault geometry in several ways.

[1] First, the plunges of the GPS coseismic displacements at the land surface are statistically parallel to the orientation of local bedding (Fig. 14) and hence parallel to the nearest adjacent segment of the 3D bedding-parallel fault ramp. That is, non-fault-parallel displacement components within the hanging wall are generally small. This is also illustrated in the five cross-sections, which show that the GPS vectors are approximately parallel to bedding and to the fault (Figs. 5, 6, 10 and 11). Note in Fig. 5 that the vectors above the detachment are close to horizontal but are slightly downward in the east, presumably reflecting elastic effects of an eastward termination of the coseismic dislocation. The fact that the non-fault-parallel components are generally second order suggests that net structural growth dominates the displacement field.

Recently Lave and Avouac (2000) made the interesting assumption that displacements over a geomorphic timescale on bedding-parallel thrusts should be parallel to surface bedding orientations and that local uplift rates therefore should be proportional to the sine of the local bedding dips. They were thereby able to estimate long-term slip rates (ca. 5 ka) on the Main Frontal thrust of the Himalayas based on uplifted dated terraces and local dip data. Our observation of bedding-parallel coseismic displacement vectors (Fig. 14) indicates that the Lave and Avouac assumption can be reasonable even on the timescale of a single large earthquake on a shallow fault. That is, the coseismic

displacement is dominated by net structural and geomorphic growth.

[2] Second, the displacement vectors are statistically parallel to large-scale corrugations (~5 km) in the fault surface, which are also reflected in broad undulations in strike of bedding in the hanging wall, with strike varying between −20 and +65° (Fig. 15). The mean corrugation fold axis (133°, 29°) measured from hanging wall bedding is nearly parallel to the mean GPS displacement vector (139°, 24°) and its azimuth is nearly parallel to the mean azimuth (140°) of horizontal displacements from *Spot* satellite data (Fig. 15). This direction is also approximately parallel to the maximum horizontal compression direction determined from borehole breakouts in the CLN-1 well (Suppe et al., 1985).

8. Regional structural setting of the Chelungpu thrust and Chi-Chi earthquake

We briefly present the larger structural geologic setting of the Chelungpu thrust and Chi-Chi earthquake within the western Taiwan thrust belt. The Chelungpu thrust shows complex linkages to adjacent active structures.

To the west of the Chelungpu ramp is the Pakuashan frontal anticline (Fig. 1) lying above the Changhua blind thrust ramp, which has been imaged in published and unpublished seismic lines (published line *G* of Chen (1978) and unpublished line *I* of Hung and Suppe (2002)). These seismic lines and surface geology and morphology display the distinctive geometric characteristics of simple-shear fault-bend folds, which are formed above thrust ramps that terminate downward in bedding-parallel detachment zones of significant thickness relative to their displacement (Jordan and Noack, 1992; Suppe et al., 2004). These diagnostic characteristics include a very long (~6–7 km) back limb with gentle dip (~10°) that dips significantly less than the ramp dip (15–20°), a narrow front limb (~2 km, 15–20°) and evidence of progressive back-limb rotation from seismic images and tilting of terraces (Ota et al., 2002). The composite regional section crossing the Pakuashan and Chelungpu structures shown in Figs. 5 and 16A is based on two seismic lines separated about 5–7 km (lines *H* and *I*, Fig. 1) and also the TSK-1 and TC-1 wells. Approximately, 2.5 km of slip (measured in the azimuth of the seismic line *I*) is consumed in the Pakuashan anticline through 60–80° of simple shear in a 770-m-thick zone in the basal Cholan Formation and Chinshui Shale, which forms the link between the Pakuashan structure and the Chelungpu ramp and detachment.

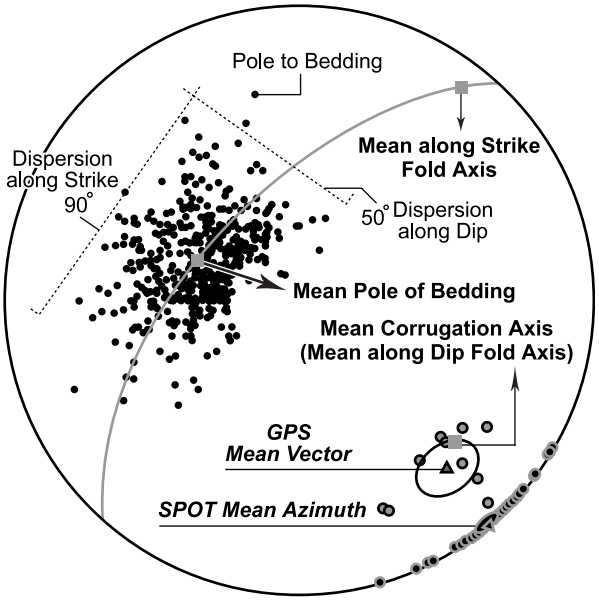

Fig. 15. Parallelism of coseismic surface displacements of the 1999 Chi-Chi earthquake with large-scale hanging wall corrugation fold axis, based on surface dip measurements above the Chelungpu ramp. Lambert's projection of poles to bedding in the hanging wall of the Chelungpu thrust ramp (segments *b–h* of Fig. 12D). The dispersion of bedding reflects two sources: [1] folding about the corrugation axis (~85° largely strike dispersion) and [2] up-dip steepening of the thrust ramp (~50° largely dip dispersion). Also see text for details.

Based on the preserved length of the seismically imaged hanging wall detachment of the Chelungpu thrust, the Chinshui detachment must extend a minimum of 14 km east of the base of Chelungpu ramp. The Shuangtung thrust to the east brings up pre-Chinshui strata, therefore the Chelungpu detachment must terminate in a major thrust ramp that extends down toward the Taiwan Main detachment, which is at a depth of approximately 10~12 km based on illumination from microseismicity as shown in Figs. 16–18 (Carena et al., 2002; also see Hirata et al., 2000; Nagai et al., 2001; Chen et al., 2002). This deep ramp appears to have been illuminated by one major aftershock of the Chi-Chi sequence (Chen et al., 2002; Kao et al., 2002; event 1 Figs. 16 and 17, $M_w = 6.16$, estimated rupture area 110–140 km^2 based on the empirical relations of Wells and Coppersmith (1994)).

The Taiwan Main detachment extends under the entire Taiwan mountain belt, diving into the mantle under eastern Taiwan (Carena et al., 2002). This detachment is illuminated by microseismicity in the vicinity of our section (Figs. 16A and 17) as far west as the Chelungpu thrust ramp, showing that the two detachments are currently operating in parallel, separated by ~7 km vertically. The Chi-Chi main shock hypocenter is located within this cloud of microseismicity, but has dipping nodal planes as shown by the first-motion focal mechanism with nodal planes dipping 34 and 56° (Chang et al., 2000; Figs. 5B, 16A and 17). Slip models suggest that after 3 s of initial minor slip on this deeper largely unknown fault, activity jumped to the Chelungpu fault (Fig. 13). This fault has a location and orientation that suggests it may be functioning as a duplex fault (see inset Fig. 17 and also Appendix A), forming a link between the Taiwan Main detachment and the Chinshui detachment. In addition, one major aftershock has an

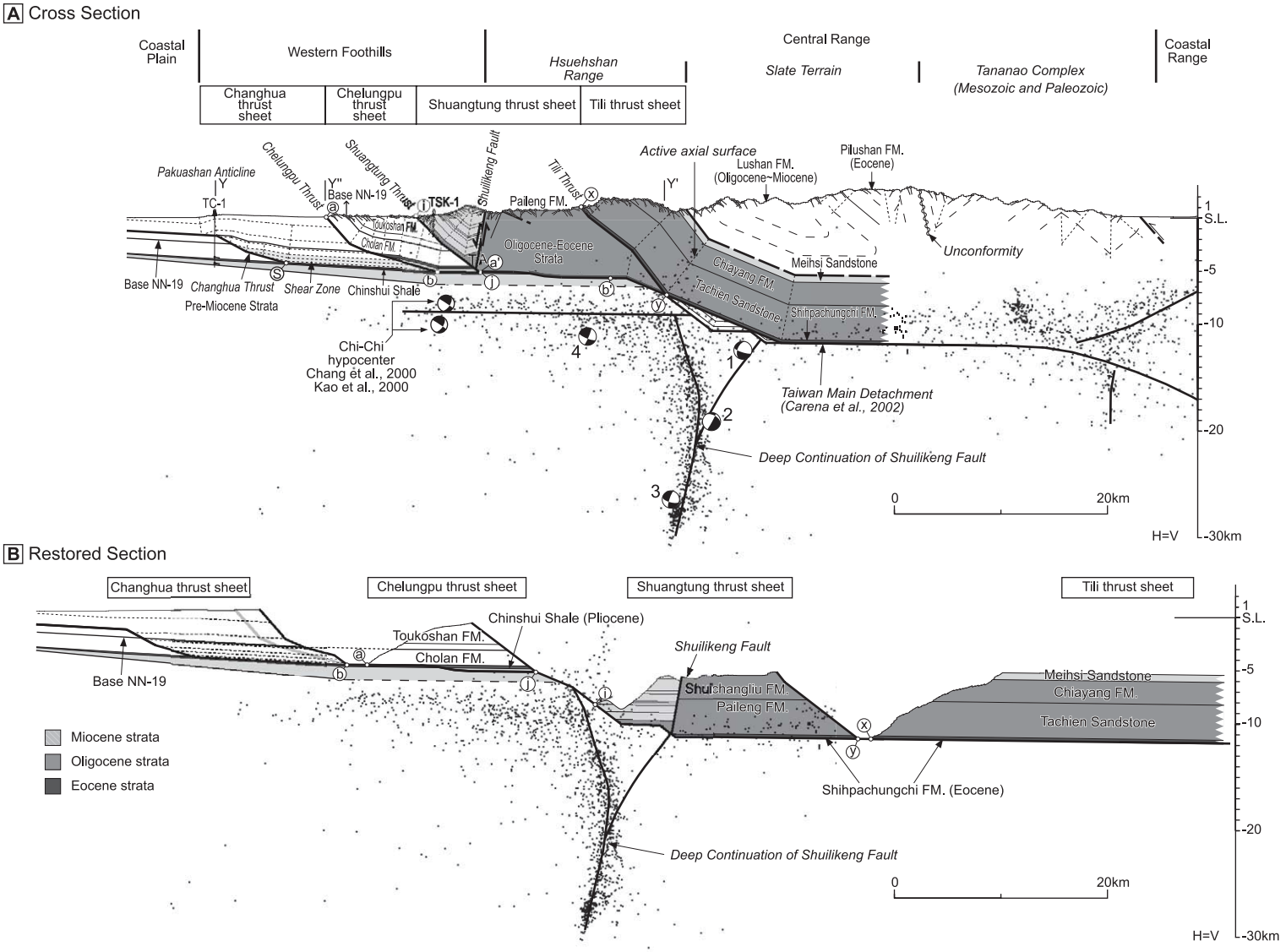

Fig. 16. Regional restoration of the Chelungpu thrust near the Chi-Chi main shock hypocenter (section YY′; Fig. 5). (A) The refined Chi-Chi main shock hypocentral locations are ~5–6 km below the Pliocene Chinshui Shale detachment of the Chelungpu thrust and lie within the 10~12 km deep cloud of microseismicity that illuminates the Taiwan Main detachment of Carena et al. (2002). Therefore the Chi-Chi earthquake did not start on the Chelungpu thrust, but on some unknown minor deeper fault. Section YY″ is based on local section ZZ′, which is oriented S60°W along seismic lines *H* and *I*; see Figs. 1 and 5. Major Chi-Chi aftershocks are numbered (Chen et al., 2002) and discussed in the text. The microseismicity (1991–2000) is from Carena et al. (2002), also shown in Figs. 16–19. This catalog has been clustered using the method of Nicholson et al. (2000). (B) Restored section showing the initial relationships between strata of the Changhua, Chelungpu, Shuangtung and Tili thrust sheets. The eastern thrust sheets ride on Oligocene and Eocene detachments, which are significantly deeper than the Pliocene Chinshui detachment to the west, requiring a major ramp system to connect them lying about 20 km east of the Chelungpu ramp. The thickness of the stratigraphic section in the Shuangtung thrust sheet constrains the height of this ramp, which suggests that it steps up from near or at the seismically illuminated Taiwan Main detachment of Carena et al. (2002). Also see text for discussion.

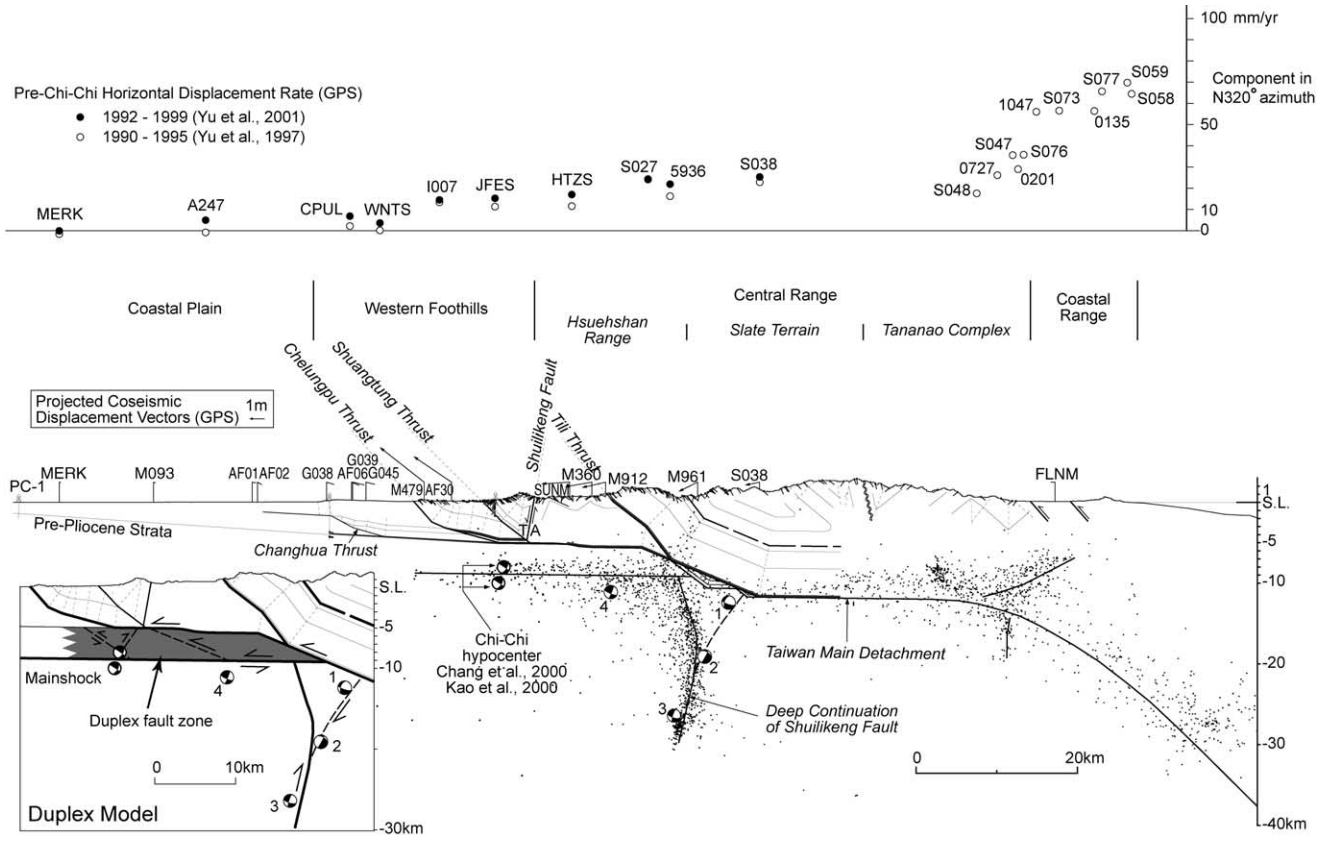

Fig. 17. Regional tectonic setting of the Chi-Chi earthquake and the Chelungpu thrust in the Taiwan mountain belt (location see inset Fig. 1). The Chelungpu thrust flattens to the Pliocene Chinshui detachment (~5–6 km) and then steps down to the seismically illuminated Taiwan Main detachment at ~10–12 km depth, which extends westward below the Chelungpu thrust. Thus the Chelungpu Chinshui Shale detachment and the Taiwan Main detachment are active in parallel. The Chi-Chi main shock and aftershock number 4 (Chen et al., 2002) are both on dipping faults that may function as duplex faults linking the parallel detachments (see inset model and text). The pre-Chi-Chi GPS observations show two regions of strong gradient in horizontal displacement rate located at the western and eastern edges of the mountainous topography, as discussed in the text (Yu et al., 1997, 2001). The coseismic GPS vectors are projected showing components of coseismic displacement in the plane of the section (station number and total displacement also given; Yu et al., 2001). The large aftershocks (1–4) were located by Chen et al. (2002) based on the joint-hypocenter method and a temporary local network; these locations are independent of the locations of background seismicity and aftershocks (1991–2000) from Carena et al. (2002).

orientation and sufficient size to be a duplex event linking the two detachments (Chen et al., 2002; event 4 Figs. 16 and 17, $M_w = 6.24$, estimated rupture area 130–160 km^2 based on the empirical relations of Wells and Coppersmith (1994)). Nevertheless imaging constraints incorporated into our cross-section require that any structural relief associated with such a duplex zone be very minor, suggesting that the Taiwan Main detachment under the Chelungpu thrust has so far accumulated only minor total displacement, leading to the speculation that it may have only recently propagated this far west.

Restoration of 2D cross-sections not only tests the validity of these sections but also provides insight into the total fault displacement and the pre-faulting geology. We present one representative restored section (Fig. 16B). Particles *a*, *i* and *x* in Fig. 16A mark the intersections of the eroded hanging walls of the Chelungpu, Shuangtung and Tili thrusts with the present land surface (Fig. 16A). These particles must restore to the east of the bases of their respective ramps, which are the footwall wall cutoff points *b*, *j* and *y*, respectively (Fig. 16A and B). Therefore, the minimum fault slips in the plane of the section relative to the foreland are [a] Chelungpu thrust: 14–16 km, [b] Shuangtung thrust: 26 km, [c] Tili thrust: >40 km. The Chelungpu–Changhua thrust sheets contain a Plio-Pleistocene stratigraphic sequence from the Chinshui Shale up to the Toukoshan Formation. In contrast, the Shuangtung and Tili thrust sheets contain a substantially older Eocene to Miocene stratigraphic sequence from the Shihpachungchi up to the Chiayang and Shuichangliu Formations. This deeper stratigraphic level east of the Shuangtung thrust requires a footwall ramp between the Chelungpu Chinshui detachment and the Oligocene and Eocene detachments of the eastern thrust sheets. Restoration indicates that the Eocene detachment is approximately at the level of the microseismically illuminated Taiwan Main detachment based on the stratigraphic thickness between the Eocene and Pliocene Chinshui detachments (Fig. 16B).

The Shuilikeng fault is a N–S sub-vertical fault, straight in map view, which was active during Miocene rifting with

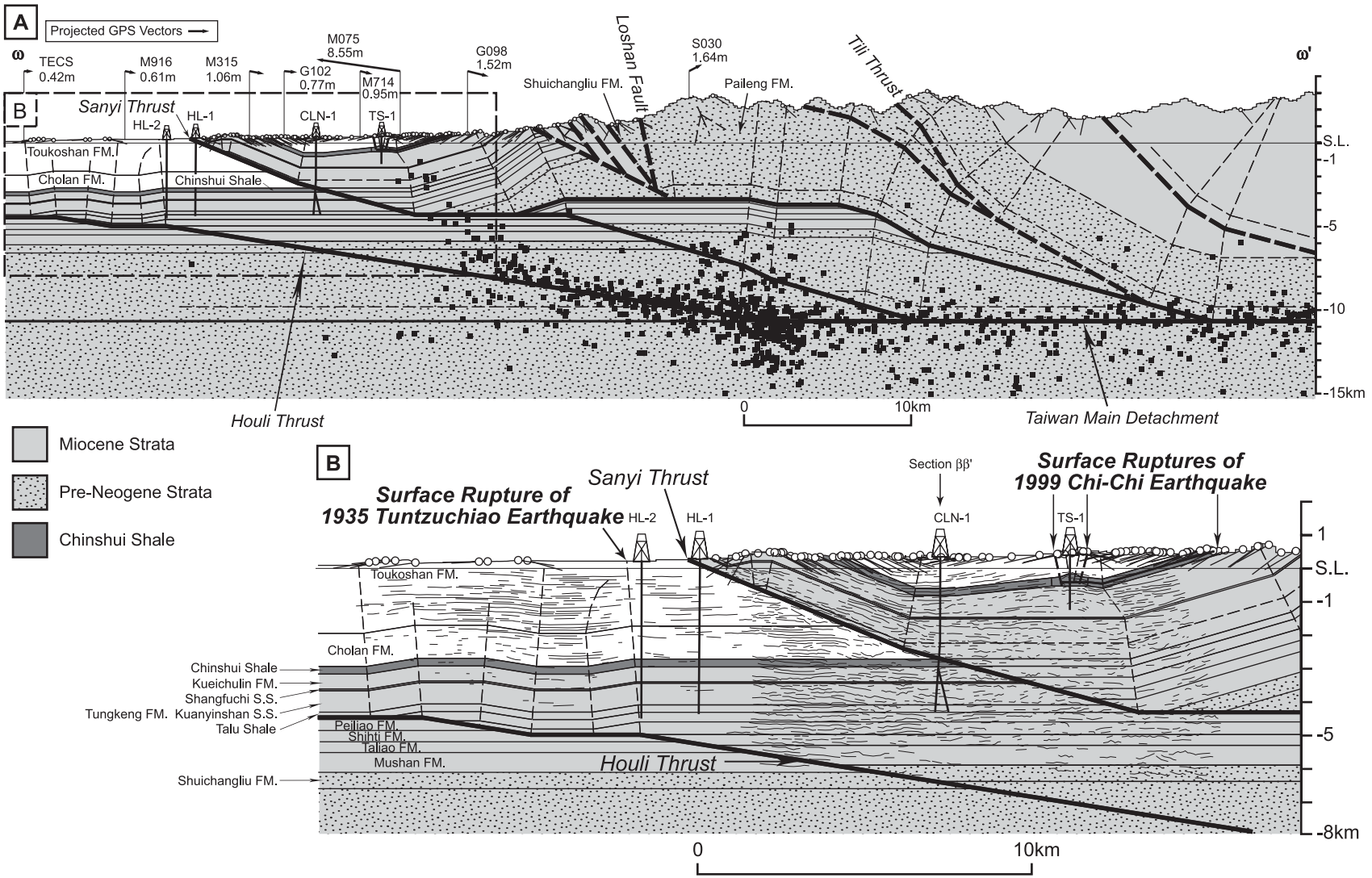

Fig. 18. Regional EW section ωω′ passing through the northernmost surface rupture of the Chi-Chi earthquake and the surface rupture of the 1935 Tuntzuchiao earthquake (location in Fig. 1). The section is constrained by seismic lines *B* and *D* (line tracings of reflectors shown in (B)), wells, surface mapping and microseismicity (black dots; Carena et al., 2002). The 1999 Chi-Chi surface ruptures are associated with surface folding of the Tungshih anticline (TS-1) above the northern termination of the shallow Chelungpu Chinshui detachment and minor surface rupture where the detachment outcrops to the east. The coseismic GPS vectors are projected showing the component of coseismic displacement in the plane of the section, which is oriented about 45° to the displacement azimuth (station number and total displacement also given; Yu et al., 2001). The 1935 Tuntzuchiao earthquake ($M_L = 7.1$) surface rupture runs in map view (Fig. 1) along the trace of the anticlinal axial surface of the kink band west of well HL-2 as constrained by seismic lines *B* and *D*; therefore, the surface rupture appears to be a fold scarp rather than a fault.

E–W Miocene normal faults abutting against it (Chinese Petroleum Corporation, 1982). We interpret this as one of the NS tear faults (transform or compartment faults) of the rifted Chinese margin (cf. Suppe, 1988). This fault in cross-section approximately lines up after restoration with a steep fault illuminated by seismicity to a depth of 30 km, including two of the major aftershocks of the Chi-Chi earthquake (Chen et al., 2002; events 2 and 3 Figs. 16 and 17, $M_w = 4.93, 5.66$, estimated rupture areas 30–40 km^2 and 4–7 km^2, respectively, based on the empirical relations of Wells and Coppersmith (1994)). In other words, the Shuilikeng fault can be seen as a major old fault that has been brought up with the Shuangtung thrust sheet, with its footwall continuation now reactivated in compression (Figs. 16 and 17). The deep Chelungpu/Shuangtung thrust ramp is localized at the heterogeneity surrounding the Oligo–Miocene Shuilikeng fault.

Our regional cross-section of Taiwan (Fig. 17) includes a comparison between decade-long pre-Chi-Chi GPS displacement rates (1990–1999) (Yu et al., 1997, 2001), which illuminates the active tectonic setting of the Chi-Chi earthquake. The main feature of the decade long GPS observations is the existence of regions of strong gradient in displacement rate on the eastern and western edges of the mountainous topography: [1] in the region of the western thrust belt, including Chelungpu fault there is a gradient of about 10 mm/yr (approximately 0–10 mm/yr) and [2] across the boundary between the Coastal Range and the eastern Central Mountains there is a gradient of about 40 mm/y (approximately 20–60 mm/yr). These data suggest that the thrust belt of the central part of western Taiwan is presently consuming only a small fraction of the present total plate convergence of ~70 mm/yr (Seno, 1977; Seno et al., 1993) in contrast to a rate of 20–40 mm/yr in the frontal thrust belt of southwestern Taiwan (Yu et al., 1997) and a rate of zero in northernmost Taiwan. This strong N–S gradient in present shortening rate in the western Taiwan thrust belt reflects the progressive turning off of oblique arc–continent collision and the plate kinematics of flipping polarity of subduction in Taiwan (see Suppe, 1984).

This regional geodetic displacement-rate profile has been modeled successfully with a creeping subhorizontal creeping detachment under the central mountains (Loevenbruck et al., 2001, 2004). This is consistent with the observation of a microseismically illuminated Taiwan Main detachment (Carena et al., 2002). Creeping faults such as the San Andreas are microseismically illuminated.

9. Relationship between the 1999 Chi-Chi and 1935 Tuntzuchiao earthquakes

In a regional sense the northern termination of the 85 km long 1999 Chi-Chi rupture ($M_w = 7.6$) marks the southern termination of the 65 km long rupture on the 1935 Tuntzuchiao earthquake ($M_L = 7.1$) as shown in the inset of Fig. 1 (Bonilla, 1975). As such it marks a major active segment boundary in the historic record of seismicity of the western Taiwan thrust belt. Here we comment briefly on the structural relationships between these two major earthquakes, making use of the cross-section of Fig. 18.

This cross-section contains the northernmost surface breaks of the Chi-Chi earthquake and is oriented strongly oblique to the coseismic surface displacement vectors (Fig. 8). The orientation and location of the cross-section was determined by the locations of seismic lines and wells. Here the North Chelungpu Chinshui Shale detachment has accumulated a total slip of less than a kilometer. Nearly all the displacement on the Sanyi–Chelungpu thrust system in this region lies on the deeper Sanyi thrust, which rides on a Miocene detachment between the Tungkeng and Kuanyinshan Formations. As discussed above, these two fault branches merge southward to become a single fault running on the Chinshui Shale detachment (Fig. 11). The Sanyi thrust does not appear to be highly active and is possibly inactive based on the lack of an active geomorphic scarp.

A deeper blind thrust ramp with minor total displacement lies below the Sanyi thrust and is presently uplifting it (1.4–4.5 km fault slip measured in seismic lines A–C). This fault is here called the Houli thrust because the active kink-band at the top of the ramp is present at Hou-Li (Nei-Pu) just west of the Sanyi thrust in Fig. 18. The southernmost 20 km of the 60-km-long surface break of the major 1935 Tuntzuchiao earthquake ($M_L = 7.1$) lies along the surface trace of the anticlinal axial surface of this kink band and showed both dip-slip and strike-slip motion, which is consistent with oblique slip on the ramp. Therefore it is likely that the southernmost portion of the 1935 earthquake ruptured the Houli blind thrust with the surface rupture being a fold scarp. The dip of the Houli ramp was computed from the dip of bedding in the kink-band and projects down dip to merge with a zone of microseismicity below 7 km that illuminates a thrust ramp that steps up from the Taiwan Main detachment at about 11 km depth. This thrust ramp, as illuminated by microseismicity, extends at least 40 km north of our cross-section, which is consistent with the large magnitude of the 1935 earthquake. Thus the Houli thrust is apparently the main active thrust in this region, although possibly the Sanyi thrust or more interior thrusts could have some activity (Fig. 18).

10. Discussion and conclusions

We have developed a 3D model of the Chelungpu–Sanyi thrust system and cross-sectional models of the western Taiwan thrust belt in the region of the 1999 Chi-Chi earthquake ($M_w = 7.6$). The largest coseismic displacements are on this thrust system. These structural models have been developed using standard structural geologic techniques based on surface geology, seismic lines, well data and balancing concepts and are largely independent of geodetic

and seismologic data from the Chi-Chi earthquake and its aftershock sequence. These structural models provide a framework that allows us to assimilate the geodetic and seismologic data into a more realistic image of this classic thrust-belt earthquake than is provided by normal earthquake studies alone. In particular, we have shown that details of the coseismic displacement fields determined from geodesy and seismology correlate significantly with fine details of the 3D fault map of the Chelungpu thrust and that to first order the displacement vectors are parallel to the fault.

The Chi-Chi earthquake is a complex rupture involving slip on a number of linked faults. A similar complexity is documented for a number of other large earthquakes, for example, Izmit (Bürgmann et al., 2002), Landers (Freymueller et al., 1994), and 1935 Tuntzuchiao (Fig. 1 inset). The rupture of Chi-Chi earthquake north of the main shock hypocenter involved at least five interlinked faults: a poorly known deep thrust where slip initiated (Fig. 17), the Chelungpu ramp, the newly propagated North Chelungpu detachment, and apparently the Chelungpu detachment and the Sanyi detachment east of the Shuangtung thrust, to judge from the geodesy. The rupture southward from the main shock hypocenter has not been studied by us in the subsurface but surface breaks indicate that it also involves several faults, including the apparently strike-slip Luliao fault and the Tachienshan thrust (Hung et al., 2002; Y.H. Lee et al., 2002).

It is clear that the Chi-Chi earthquake is not a characteristic earthquake for the Chelungpu thrust system in the sense that repetitions of this event do not sum to the total displacement field of this thrust system, even on a relatively short term basis. Slip magnitude is highly heterogeneous, both within the Chelungpu ramp and between the ramp and Chinshui detachment. Other substantial earthquakes with different slip distributions must make up the difference or there must be substantial creep, particularly on the detachment. However, major creeping faults such as the San Andreas are illuminated by substantial microseismicity, which has not been observed on the Chelungpu fault either before or after the Chi-Chi earthquake (Fig. 19). In contrast, the Taiwan Main detachment and the deeper Houli ramp are illuminated by microseismicity and it has been argued that Taiwan Main detachment is creeping under the Central Mountains based on modeling of geodetic data (Loevenbruck et al., 2001, 2004). Therefore the mode of displacement on the Chinshui Shale detachment is an open question.

The distribution of seismicity surrounding the Chelungpu thrust shows broadly similar patterns pre- and post-Chi-Chi, with the region that slipped in the Chi-Chi earthquake being nearly devoid of small-to-moderate earthquakes (less than 20 events in the upper 7 km; Fig. 19A), but the adjacent regions show dense seismicity. This extremely low background and aftershock seismicity for the Chelungpu thrust suggests that the fault may be locked during the interseismic period.

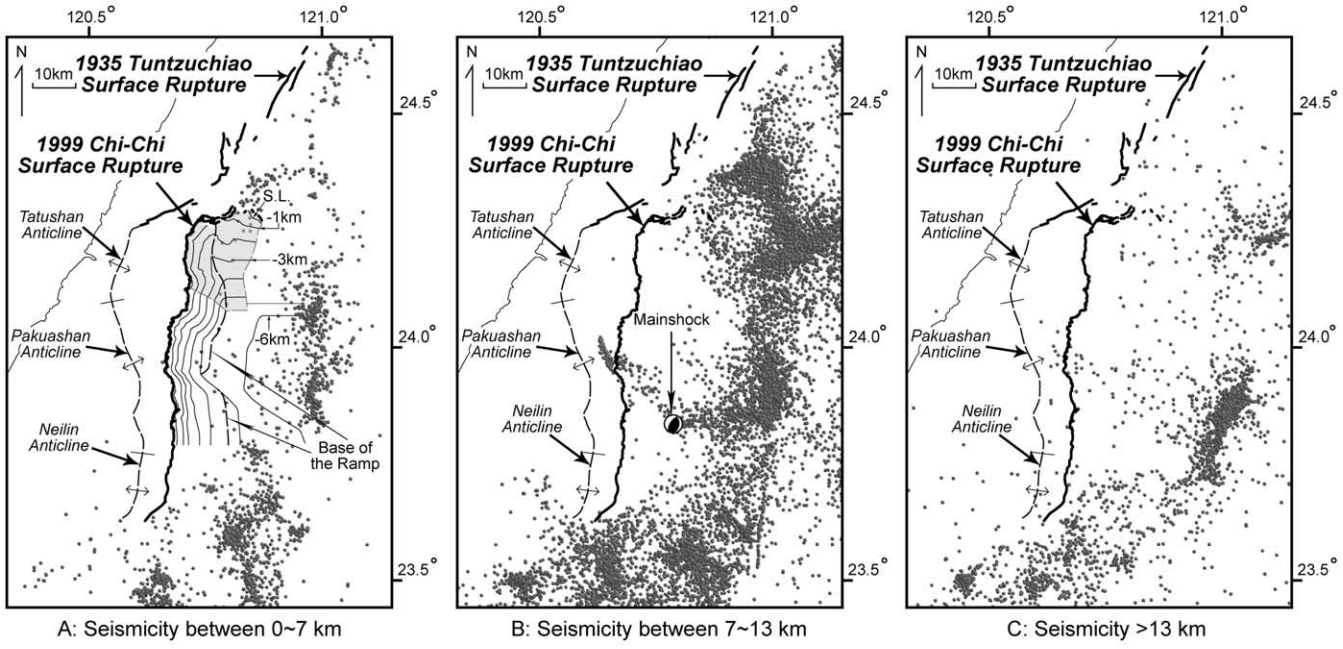

Fig. 19. Background and aftershock seismicity (1991–2000) (Carena et al., 2002) showing a lack of microseismicity on the Chelungpu ramp and detachment, which suggests that they are not creeping (see text). (A) 0∼7 km. There is a near lack of seismicity in the vicinity of the Chelungpu thrust ramp and Chinshui Shale detachment (only ∼20 events). Those few events are somewhat concentrated near the base of the ramp. The dense seismicity to the east is located around the deep ramp of the Chelungpu thrust, which is seen more strongly in the 7∼13 km interval. The linear cluster of seismicity along the NE extension of the northernmost 1999 surface rupture is associated with the up-dip termination of the creeping section of the Houli thrust (see Fig. 18). (B) 7∼13 km. Seismicity below the Chelungpu thrust and within ±3 km of the Taiwan Main detachment. The Chi-Chi main shock hypocenter is associated with a NW-trending cluster of microseismicity within the larger Taiwan Main detachment (see also Fig. 17). (C) >13 km. Seismicity below the Taiwan Main detachment.

The large difference in total slip between the North Chelungpu Chinshui detachment (~0.3 km) and the main Chelungpu ramp and detachment (~15 km) might imply different fault-zone structure and mechanical behavior for these distinct segments of the Chelungpu–Sanyi system (Fig. 9). Here we comment briefly on the proposal of Brodsky and Kanamori (2001) and Ma et al. (2003) that the northern high-slip portion of the Chi-Chi earthquake may display hydrodynamic frictional weakening based on analysis of the unusual lack of high-frequency radiation seen in two broad-band strong-motion instruments directly above the fault (stations TCU052 and TCU068 in Fig. 20). Regardless of whether or not hydrodynamic friction was in operation we note that this segment of the fault lies along the newly-propagated North Chelungpu Chinshui detachment, which is parallel to bedding above and below and shows a total slip of only ~0.3 km (~35 Chi-Chi events), which is consistent with smooth rupture. In contrast the cross-cutting Chelungpu ramp to the south, which has ~15 km total slip (3000–5000 Chi-Chi earthquakes), showed substantial high-frequency radiation in near-field stations (stations TCU067, TCU075 and TCU129 in Fig. 20), which is consistent with a more complex and heterogeneous fault zone and rupture process. The Taiwan Chelungpu-Fault Drilling Project (TCDP) (2003) is currently drilling a scientific borehole through the high-slip northern portion of the fault and through the Sanyi ramp in the footwall, which should supply new data on fault-zone structure (Figs. 1, 2, 9 and 10).

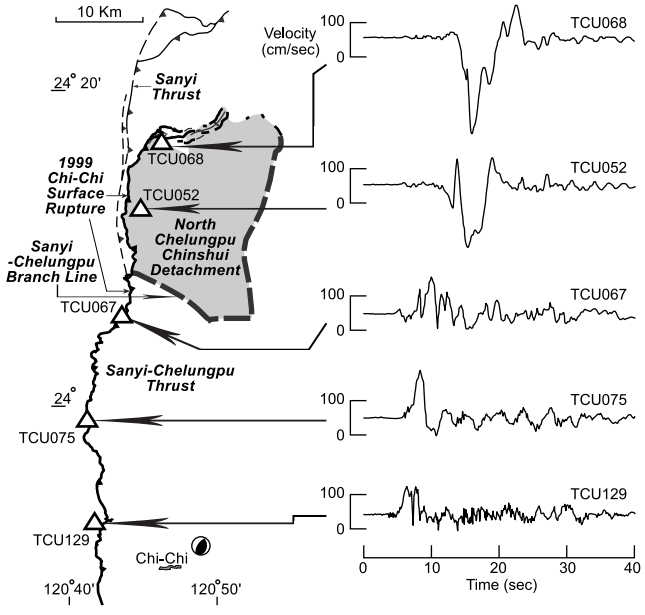

Fig. 20. The E–W component of velocity strong-motion seismograms for five stations near the 1999 Chi-Chi surface rupture. Note that the northernmost two stations associated with the North Chelungpu Chinshui detachment, TCU052 and TCU068, have much less high frequency content, which suggests a much smoother rupture dynamics in contrast with the three stations to the south on the main Sanyi–Chelungpu ramp (Ma et al., 2003). In addition Ma et al. (2003) have proposed that the smooth slip in the north may be associated with hydrodynamic weakening.

This study of the Chi-Chi earthquake shows the value of normal subsurface structural geologic techniques in illuminating the meaning of much geodetic and seismologic data obtained in studies of well-instrumented earthquakes. These and similar studies (for example Shaw and Shearer, 1999; Allmendinger and Shaw, 2000; Rivero et al., 2000; Carena and Suppe, 2002) illustrate the growing opportunities that exist at the interface between structural geology and earthquake seismology, which is a natural interface, given the fact that large earthquakes are the quanta of much upper-crustal structural growth.

Acknowledgements

We are grateful for the very thoughtful reviews of the manuscript by Jean-Philippe Avouac of Caltech, Karl Mueller of University of Colorado and John Stamatakos of CNWRA at Southwest Research Institute. We are particularly grateful to Ching-Hua Lo and Yue-Gau Chen of National Taiwan University and Yuan-Hsi Lee of National Chung Cheng University for their hospitality and support of this work. We are especially grateful to the Chinese Petroleum Company for their hospitality and for access to data needed for our structural models. We thank the National Science Council for financial support for field work. We are grateful to Stéphane Dominguez and Jean-Philippe Avouac for access to their fundamental paper in advance of publication. We thank Honn Kao of the Geological Survey of Canada and Sara Carena of Princeton University for their help at many stages in this project. Fig. 15 was produced using stereo software of Rick Allmendinger.

Appendix A. Alternative connections between the Chelungpu fault and the main shock hypocenter

There has been a natural tendency in many geophysical and geologic studies of the Chi-Chi earthquake to directly interpolate a simple dipping fault between the main-shock hypocenter at 8–10 km and the surface break on the Chelungpu thrust (e.g. Fig. 13). Nearly all of these interpolations are inconsistent with the compelling evidence summarized above that the Chelungpu–Sanyi thrust ramp flattens to a much shallower detachment, which is 5–6 km deep in the vicinity of the main-shock hypocenter. Furthermore the observed Chi-Chi slip distribution (Figs. 12 and 13) would be unusual for a simple fault running directly from 10 km to the surface because well-resolved large slip is shallower than 6 km rather than deep. Therefore such a simple fault geometry for the Chi-Chi rupture seems implausible.

Nevertheless it is possible to develop a self-consistent cross-section through the hypocenter that does have a relatively direct connection between the hypocenter and the

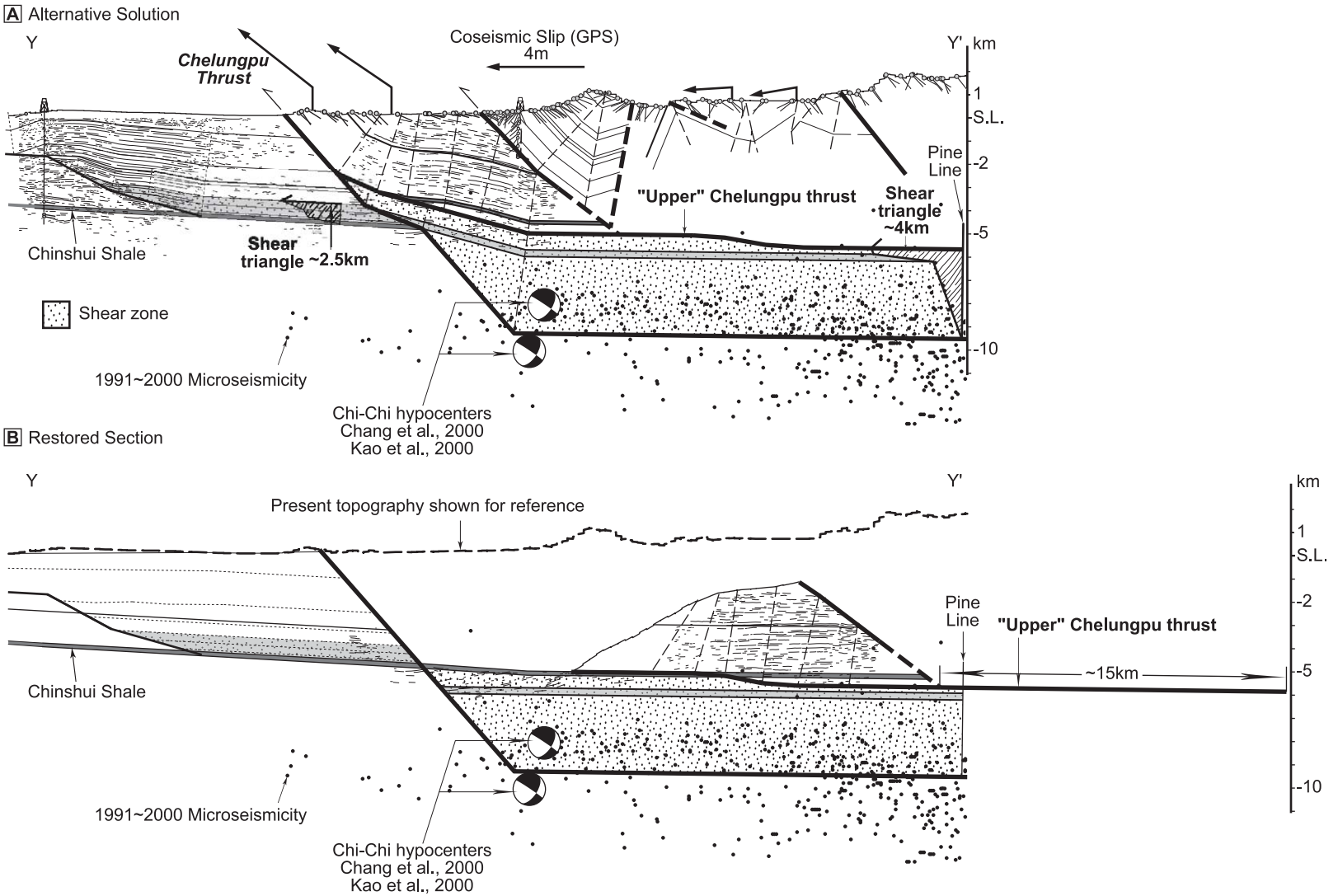

Fig. 21. (A) An alternative fault model that attempts to form a self-consistent direct interpolation between the Chi-Chi main shock hypocenter and the surface rupture on the Chelungpu thrust, similar to many of the geophysical models of the Chi-Chi earthquake (e.g. Fig. 13). Such a hypothesized through-going fault would be complex because it must be mutually cross-cutting with the Chinshui Shale detachment, which is also presently active in the Chelungpu and Changhua structures. The part of such a ramp cutting the Chinshui Shale could only have minor slip because the Chinshui shale is at similar elevations across this hypothesized ramp (Fig. 4). (B) Restoration of this alternative model requires about 15 km total slip for the Chelungpu thrust.

surface break (Fig. 21). This necessarily involves slip on two mutually cross-cutting fault systems, both of which are active: (1) the Pliocene Chinshui Shale detachment, which is active in both the Chelungpu and Changhua thrusts, and (2) the hypothesized through-going fault ramp connecting directly from the hypocenter to the surface break. This deep-ramp model cannot be easily extended to the north along the Chelungpu–Sanyi system (Figs. 5, 10 and 11) and could not have substantial total slip on the deep ramp given the similar elevations of the Chinshui Shale across the fault (Fig. 4). There is no compelling evidence for the solution of Fig. 21. Given the limited deep constraints we prefer to remain agnostic as to the details of the deep fault geometry. We show one plausible duplex solution in Fig. 17 (inset) in which the fault of the deep hypocenter is minor and does not cut across the Chinshui Shale detachment.

References

Allmendinger, R., Shaw, J.H., 2000. Estimation of fault-propagation distance from fold shape: implications for earthquake hazards assessment. Geology 28, 1099–1102.

Bonilla, M.G., 1975. A review of recently active faults in Taiwan. United States Department of the Interior Geological Survey, Open-File Report, 75–41, 58pp.

Brodsky, E.E., Kanamori, H., 2001. Elastohydrodynamic lubrication of faults. Journal of Geophysical Research 106, 16357–16374.

Bürgmann, R., Ergintav, S., Segall, P., Hearn, E.H., McClusky, S.C., Reilinger, R.E., Woith, H., Zschau, J., 2002. Time-dependent distributed afterslip on and deep below the Izmit earthquake rupture. Bulletin of the Seismological Society of America 92, 126–137.

Carena, S., Suppe, J., 2002. 3-D Imaging of active structures using earthquake aftershocks: the Northridge thrust, California. Journal of Structural Geology 24, 887–904.

Carena, S., Suppe, J., Kao, H., 2002. The active detachment of Taiwan illuminated by small earthquakes and its control of first-order topography. Geology 30, 935–938.

Central Geological Survey, 1999a. Report of the geological survey of the 1999 Chi-Chi earthquake. Central Geological Survey, Ministry of Economic Affairs, ROC (in Chinese).

Central Geological Survey, 1999b. Map of surface ruptures along the Chelungpu fault during the Chi-Chi earthquake, Taiwan. Central Geological Survey, Ministry of Economic Affairs, ROC, scale 1:25,000.

Chang, C.H., Wu, Y.M., Shin, T.C., Wang, C.Y., 2000. Relocation of the 1999 Chi-Chi Earthquake in Taiwan. Terrestrial. Atmospheric and Oceanic Sciences 11, 581–590.

Chang, H.C., 1994. Geological map of Taiwan, Ta-Chia. Central Geological Survey Sheet 17, scale 1:50,000.

Chang, S.S.L., 1971. Subsurface geologic study of the Taichung Basin, Taiwan. Petroleum Geology of Taiwan 8, 21–45.

Chen, J.S., 1978. A comparative study of the refraction and reflection seismic data obtained on the Changhua plain to the Peikang shelf, Taiwan. Petroleum Geology of Taiwan 15, 199–217.

Chen, K.C., Huang, B.S., Wang, J.H., Yen, H.Y., 2002. Conjugate thrust faulting associated with the 1999 Chi-Chi, Taiwan, earthquake sequence. Geophysical Research Letters 29 (8), 1277. doi:10.1029/2001GL014250.

Chinese Petroleum Corporation, 1968. Geologic map of Chelungpu structure, Tai-Chung. Taiwan Petroleum Exploration Division, Chinese Petroleum Corporation, ROC, scale 1:25,000.

Chinese Petroleum Corporation, 1974. Geological map of Miao-Li. Taiwan Petroleum Exploration Division, Chinese Petroleum Corporation, ROC, scale 1:100,000.

Chinese Petroleum Corporation, 1982. Geological map of Tai-Chung. Taiwan Petroleum Exploration Division, Chinese Petroleum Corporation, ROC, scale 1:100,000.

Dahlen, F.A., Suppe, J., Davis, D., 1984. Mechanics of fold-and-thrust belts and accretionary wedges: cohesive Coulomb theory. Journal of Geophysical Research 89, 10087–10101.

Dominguez, S., Avouac, J.P., Michel, R., 2003. Horizontal coseismic deformation of the 1999 Chi-Chi earthquake measured from Spot satellite images: Implications for the seismic cycle along the western foothills of central Taiwan. Journal of Geophysical Research 108 (B2), 2083. doi:10.1029/2001JB000951.

Freymueller, J., King, N.E., Segall, P., 1994. The co-seismic slip distribution of the Landers earthquake. Bulletin of the Seismological Society of America 84, 646–659.

Hartzell, S.H., Stewart, G.S., Mendoza, C., 1991. Comparison of L_1 and L_2 norms in a teleseismic waveform inversion for the slip history of the Loma Prieta, California, earthquake. Bulletin of the Seismological Society of America 81 (5), 1518–1539.

Hirata, N., Sakai, S., Liaw, Z.S., Tsai, Y.B., Yu, S.B., 2000. Aftershock observations of the 1999 Chi-Chi, Taiwan earthquake. Bulletin of Earthquake Research Institute of Tokyo University 75, 33–46.

Ho, H.C., Chen, M.M., 2000. Geological map of Taiwan, Tai-Chung. Central Geological Survey Sheet 24, scale 1:50,000.

Hsu, Y.J., Bechor, N., Segall, P., Yu, S.B., Kuo, L.C., Ma, K.F., 2002. Rapid afterslip following the 1999 Chi-Chi, Taiwan earthquake. Geophysical Research Letters 29 (16), 1754. doi:10.1029/2002GL014967.

Hu, C.C., Chiu, H.T., 1984. Deep structures of the Cholan area, Northwestern Taiwan. Petroleum Geology of Taiwan 20, 21–33.

Huang, C.S., Shea, K.S., Chen, M.M., 2000. Geological map of Taiwan, Pu-Li. Central Geological Survey Sheet 32, scale 1:50,000.

Hung, J., Suppe, J., 2002. Subsurface Geometry of the Sanyi–Chelungpu Faults and Fold Scarp Formation in the 1999 Chi-Chi Taiwan Earthquake. Eos, Transactions, American Geophysical Union 83 (47, suppl.), T61B-1268.

Hung, J.H., Wiltschko, D.V., 1993. Structure and kinematics of arcuate thrust faults in the Miaoli–Cholan area of western Taiwan. Petroleum Geology of Taiwan 28, 59–96.

Hung, J.H., Zhan, H.P., Wiltschko, D.V., Fang, P., 2002. Geodetically observed surface displacements of the 1999 Chi-Chi earthquake near southern termination of the Chelungpu fault. Terrestrial, Atmospheric and Oceanic Sciences 13, 355–366.

Ide, S., Takeo, M., 1997. Determination of constitutive relations of fault slip based on seismic wave analysis. Journal of Geophysical Research 102, 27379–27391.

Ji, C., Helmberger, D.V., Song, T.R.A., Ma, K.F., Wald, D.J., 2001. Slip distribution and tectonic implication of the 1999 Chi-Chi, Taiwan, earthquake. Geophysical Research Letters 28, 4379–4382.

Ji, C., Helmberger, D.V., Wald, D.J., Ma, K.F., 2003. Slip history and dynamic implications of the 1999 Chi-Chi, Taiwan, earthquake. Journal of Geophysical Research 108 (B9), 2412. doi:10.1029/2002JB001764.

Johnson, K.M., Segall, P., 2003. Imaging the ramp-decollement geometry of the Chelungpu fault using coseismic GPS displacements from the 1999 Chi-Chi, Taiwan earthquake. Tectonophysics 378, 123–139.

Johnson, K.M., Hsu, Y.J., Segall, P., Yu, S.B., 2001. Fault geometry and slip distribution of the 1999 Chi-Chi, Taiwan earthquake imaged from inversion of GPS data. Geophysical Research Letters 28, 2285–2288.

Jordan, P., Noack, T., 1992. Hangingwall geometry of overthrusts emanating from ductile decollements. In: McClay, K. (Ed.), Thrust Tectonics. Chapman and Hall, London, pp. 311–318.

Kao, H., Chen, R.Y., Chang, C.H., 2000. Exactly where does the 1999 Chi-Chi earthquake in Taiwan nucleate? Hypocenter relocation using the master station method. Terrestrial, Atmospheric and Oceanic Sciences 11, 567–580.

Kao, H., Liu, Y.H., Liang, W.T., Chen, W.P., 2002. Source parameters of regional earthquakes in Taiwan: 1999–2000 including the Chi-Chi earthquake sequence. Terrestrial, Atmospheric and Oceanic Sciences 13, 279–298.

Kaverina, A., Dreger, D., Price, E.J., 2002. The combined inversion of seismic and geodetic data for the source process of the 16 October 1999 M_w 7.1 Hector Mine, California, earthquake. Bulletin of the Seismological Society of America 92, 1266–1280.

King, G.C., Stein, R.S., Rundle, J.B., 1988. The growth of geologic structures by repeated earthquakes. I. Conceptual framework. Journal of Geophysical Research 93, 13307–13318.

Lave, J., Avouac, J.P., 2000. Active folding of fluvial terraces across the Siwaliks Hills, Himalayas of central Nepal. Journal of Geophysical Research 105, 5735–5770.

Lee, J.C., Chu, H.T., Angelier, J., Chan, Y.C., Hu, J.C., Lu, C.Y., Rau, R.J., 2002. Geometry and structure of northern surface ruptures of the 1999 $M_w = 7.6$ Chi-Chi Taiwan earthquake: influence from inherited fold belt structures. Journal of Structural Geology 24, 173–192.

Lee, J.F., 2000. Geological map of Taiwan, Tung-Shih. Central Geological Survey Sheet 18, scale 1:50,000.

Lee, P.J., 1962. Mesozoic and Cenozoic rocks of the Paochung well, Yunlin, Taiwan. Petroleum Geology of Taiwan 1, 75–86.

Lee, Y.H., Wu, W.Y., Shih, T.S., Lu, S.D., Hsieh, M.L., Chen, H.C., 2000. Deformation characteristics of surface ruptures of the Chi-Chi earthquake, east of the Pifeng Bridge. Central Geological Survey, Special Publication 12, 9–40.

Lee, Y.H., Lu, S.D., Shih, T.S., 2002. Deformation mechanism of the southern ending of the Chi-Chi earthquake—the TFF triple-junction model. Bulletin of Central Geological Survey 15, 87–101.

Lee, Y.H., Hsieh, M.L., Lu, S.D., Shih, T.S., Wu, W.Y., Sygiyama, Y., Azuma, T., Kariya, Y., 2003. Slip vectors of the surface rupture of the 1999 Chi-Chi earthquake, western Taiwan. Journal of Structural Geology 25, 1917–1931.

Lo, W., Wu, L.C., Chen, H.W., 1999. Geological map of Taiwan, Kou-Hsing. Central Geological Survey Sheet 25, scale 1:50,000.

Loevenbruck, A., Cattin, R., Pichon, X.L., Courty, M.L., Yu, S.B., 2001. Seismic cycle in Taiwan derived from GPS measurements. Comptes Rendus de l'Académie des Sciences—Series IIA—Earth and Planetary Science 333, 57–64.

Loevenbruck, A., Cattin, R., Le Pichon, X., Dominguez, S., Michel, R., 2004. Coseismic slip resolution and post-seismic relaxation time of the 1999 Chi-Chi, Taiwan, earthquake as constrained by geological observations, geodetic measurements and seismicity. Geophysical Journal International 158, 310–326.

Ma, K.F., Lee, C.T., Tsai, Y.B., Shin, T.C., Mori, J., 1999. The Chi-Chi Taiwan earthquake: large surface displacements on inland thrust fault. Eos, Transactions, American Geophysical Union 80, 605–611.

Ma, K.F., Song, T.R.A., Lee, S.J., Wu, H.I., 2000. Spatial slip distribution of the September 20, 1999, Chi-Chi, Taiwan, earthquake (M_w 7.6): inverted from teleseismic data. Geophysical Research Letters 27, 3417–3420.

Ma, K.F., Mori, J., Lee, S.J., Yu, S.B., 2001. Spatial and temporal distribution of slip for the 1999 Chi-Chi, Taiwan, earthquake. Bulletin of the Seismological Society of America 91, 1069–1087.

Ma, K.F., Brodsky, E.E., Mori, J., Ji, C., Song, T.R.A., Kanamori, H., 2003. Evidence for fault lubrication during the 1999 Chi-Chi, Taiwan, earthquake (M_w 7.6). Geophysical Research Letters 30 (5), 1244. doi:10.1029/2002GL015380.

Mitra, S., 1988. Three-dimensional geometry and kinematic evolution of the Pine Mountain thrust system, southern Appalachians. Geological Society of America Bulletin 100, 72–95.

Nagai, S., Hirata, N., Sakai, S., Huang, B.S., 2001. Distribution and structural details of the aftershocks of the 1991 Chi-Chi, Taiwan earthquake. Eos, Transactions, American Geophysical Union 82, 1177.

Nicholson, T., Sambridge, M., Gudmundsson, O., 2000. On entropy and clustering in earthquake hypocenter distribution. Geophysical Journal International 142, 37–51.

Ota, Y., Shyu, J.B.H., Chen, Y.G., Hsieh, M.L., 2002. Deformation and age of fluvial terraces south of the Choushui River, Central Taiwan, and their tectonic implications. Western Pacific Earth Sciences 2, 251–260.

Perfettini, H., Avouac, J.P., 2004. Postseismic relaxation driven by brittle creep: a possible mechanism to reconcile geodetic measurements and the decay rate of aftershocks, application to the Chi-Chi earthquake, Taiwan. Journal of Geophysical Research 109 (B02304). doi:10.1029/2003JB002488.

Price, R.A., 2001. An evaluation of models for the kinematic evolution of thrust and fold belts: structural analysis of a transverse fault zone in the Front Ranges of the Canadian Rockies north of Banff, Alberta. Journal of Structural Geology 23, 1079–1088.

Rivero, C., Shaw, J.H., Mueller, K., 2000. The Oceanside and Thirtymile Bank thrusts: implications for earthquake hazards in coastal southern California. Geology 28, 891–894.

Roeder, D., Witherspoon, W.D., 1978. Palinspastic map of east Tennessee. American Journal of Science 278, 543–550.

Roeder, D., Gilbert, E., Witherspoon, W.D., 1978. Evolution and macroscopic structure of Valley and Ridge thrust belt, Tennessee and Virginia. University of Tennessee, Department of Geologic Science, Studies in Geology 2, 25pp.

Sekiguchi, H., Iwata, T., 2001. The source process of the 1999 Chi-Chi, Tawian, earthquake in semi-long period (2–20 s). Annual Report on Active Fault and Paleoearthquake Researches, Geological Survey of Japan 1, 315–324.

Seno, T., 1977. The instantaneous rotation vector of the Philippine Sea plate relative to the Eurasian plate. Tectonophysics 42, 209–226.

Seno, T., Stein, S., Gripp, A.E., 1993. A model for the motion of the Philippine Sea plate consistent with NUVEL-1 and geological data. Journal of Geophysical Research 98, 17941–17948.

Shaw, J.H., Shearer, P., 1999. An elusive blind-thrust fault beneath metropolitan Los Angeles. Science 283, 1516–1518.

Stein, R.S., King, G.C., 1984. Seismic potential revealed by surface folding: 1983 Coalinga, California, Earthquake. Science 224, 869–872.

Stein, R.S., King, G.C., Rundle, J.B., 1988. The growth of geologic structures by repeated earthquakes, II. Field examples of continental dip slip. Journal of Geophysical Research 93, 13319–13331.

Suppe, J., 1980. A retrodeformable cross-section of northern Taiwan. Proceedings of Geological Society of China 23, 46–55.

Suppe, J., 1984. Kinematics of arc-continent collision, flipping of subduction, and back-arc spreading near Taiwan. Geological Society of China, Memoir 6, 21–33.

Suppe, J., 1985. Principles of Structural Geology. Prentice-Hall, Englewood Cliffs, NJ. 537pp.

Suppe, J., 1988. Tectonics of arc-continent collision on both sides of the South China Sea: Taiwan and Mindoro. Acta Geologica Taiwanica 26, 1–18.

Suppe, J., Connors, C.D., Zhang, Y.K., 2004. Shear fault-bend folding. In: McClay, K.R. (Ed.), Thrust Tectonics American Association of Petroleum Geologists, Memoir, 82, pp. 303–323.

Suppe, J., Hu, C.T., Chen, Y.J., 1985. Present-day stress directions in western Taiwan inferred from borehole elongation. Petroleum Geology of Taiwan 21, 1–12.

Taiwan Chelungpu-Fault Drilling Project, 2003. TCDP Logging and Casing Plan. In: Investigating the Physics of Faulting Pre-Drilling Workshop, Taiwan Chelungpu-Fault Drilling Project (21 Oct. 2003), 11pp. {http://eqkc.earth.ncu.edu.tw/EQKCTCDP.htm}.

Wang, C.Y., 2002. Detection of a recent earthquake fault by the shallow reflection seismic method. Geophysics 67, 1465–1473.

Wang, C.Y., 2003. Review of TCDP. In: Investigating the Physics of Faulting Pre-Drilling Workshop, Taiwan Chelungpu-Fault Drilling Project (21 Oct. 2003), 21pp. {http://eqkc.earth.ncu.edu.tw/EQKCTCDP.htm}.

Wang, C.Y., Chang, C.H., Yen, H.Y., 2000. An interpretation of the 1999 Chi-Chi earthquake on Taiwan based on the thin-skinned thrust model. Terrestrial, Atmospheric and Oceanic Sciences 11, 609–630.

Wang, C.Y., Li, C.L., Su, F.C., Leu, M.T., Wu, M.S., Lai, S.H., Chern, C.C., 2002a. Structural mapping of the 1999 Chi-Chi earthquake fault, Taiwan by seismic reflection methods. Terrestrial, Atmospheric and Oceanic Sciences 13, 211–226.

Wang, C.Y., Li, C.L., Yen, H.Y., 2002b. Mapping the northern portion of the Chelungpu fault, Taiwan by shallow reflection seismics. Geophysical Research Letters 29 (16). doi:10.1029/2001GL014496.

Wang, C.Y., Tanaka, H., Chow, J., Chen, C.C., Hong, J.H., 2002c. Shallow reflection seismic aiding geological drilling into the Chelungpu fault after the 1999 Chi-Chi earthquake, Taiwan. Terrestrial, Atmospheric and Oceanic Sciences 13, 153–170.

Wang, C.Y., Kuo, S.Y., Shyu, W.L., Hsiao, J.W., 2003. Investigating near-surface structures under the Changhua fault, west-central Taiwan by the reflection seismic method. Terrestrial, Atmospheric and Oceanic Sciences 14, 343–367.

Wang, C.Y., Li, C.L., Lee, H.C., 2004. Constructing subsurface structures of the Chelungpu fault to investigate mechanisms leading to abnormally large ruptures during the 1999 Chi-Chi earthquake, Taiwan. Geophysical Research Letters 31, L02608. doi:10.1029/2003GL018323.

Wang, W.M., He, Y.M., Yao, Z.X., 2004. Complexity of the coseismic rupture for 1999 Chi-Chi Earthquake (Taiwan) from inversion of GPS observations. Tectonophysics 382, 151–172.

Wells, D.L., Coppersmith, K.J., 1994. New empirical relationships among magnitude, rupture length, rupture width, rupture area, and surface displacement. Bulletin of the Seismological Society of America 84, 974–1002.

Wu, C., Takeo, M., Ide, S., 2001. Source process of the Chi-Chi earthquake: a joint inversion of strong motion data and global positioning system data with a multifault model. Bulletin of the Seismological Society of America 91, 1128–1143.

Yeats, R.S., Sieh, K., Allen, C.R., 1996. Geology of Earthquakes. Oxford University Press, Oxford. 568pp.

Yu, S.B., Chen, H.Y., Kuo, L.C., 1997. Velocity field of GPS stations in the Taiwan area. Tectonophysics 274, 41–59.

Yu, S.B., Kuo, L.C., Hsu, Y.J., Su, H.H., Liu, C.C., Hou, C.S., Lee, J.F., Lai, T.C., Liu, C.C., Liu, C.L., Tseng, T.F., Tsai, C.S., Shin, T.C., 2001. Preseismic deformation and coseismic displacements associated with the 1999 Chi-Chi, Taiwan, earthquake. Bulletin of the Seismological Society of America 91, 995–1012.

Yu, S.B., Hsu, Y.J., Kuo, L.C., Chen, H.Y., Liu, C.C., 2003. GPS measurement of postseismic deformation following the 1999 Chi-Chi, Taiwan, earthquake. Journal of Geophysical Research 108 (B11), 2520. doi:10.1029/2003JB002396.

Zeng, Y., Chen, C.H., 2001. Fault rupture process of the 20 September 1999 Chi-Chi, Taiwan, earthquake. Bulletin of the Seismological Society of America 91, 1088–1098.